

Linear and Weakly Nonlinear Stability Analyses of Turing Patterns for Diffusive Predator–Prey Systems in Freshwater Marsh Landscapes

Li Zhang¹ · Fan Zhang² · Shigui Ruan² 

Received: 12 October 2016 / Accepted: 4 January 2017 / Published online: 30 January 2017
© Society for Mathematical Biology 2017

Abstract We study a diffusive predator–prey model describing the interactions of small fishes and their resource base (small invertebrates) in the fluctuating freshwater marsh landscapes of the Florida Everglades. The spatial model is described by a reaction–diffusion system with Beddington–DeAngelis functional response. Uniform bound, local and global asymptotic stability of the steady state of the PDE model under the no-flux boundary conditions are discussed in details. Sufficient conditions on the Turing (diffusion-driven) instability which induces spatial patterns in the model are derived via linear analysis. Existence of one-dimensional and two-dimensional spatial Turing patterns, including rhombic and hexagonal patterns, are established by weakly nonlinear analyses. These results provide theoretical explanations and numerical simulations of spatial dynamical behaviors of the wetland ecosystems of the Florida Everglades.

Keywords Reaction–diffusion predator–prey system · Beddington–DeAngelis functional response · Stability · Turing pattern · Weakly nonlinear analysis

Mathematics Subject Classification 35K57 · 35K55

Research was partially supported by National Science Foundation (DMS-1412454).

✉ Shigui Ruan
ruan@math.miami.edu

¹ School of Mathematics and Statistics, Xidian University, Xi’an 710071, Shaanxi, China

² Department of Mathematics, University of Miami, Coral Gables, FL 33146, USA

1 Introduction

The Everglades in the USA is a large contiguous wetland that has served as a model for hydrologically pulsed ecosystems with extensive wetland habitats. The assemblage of populations of small fishes, such as killifishes (*Fundulidae*), poeciliids (*Poeciliidae*), and juvenile sunfishes (*Centrarchidae*), of the freshwater marshes of the Everglades is affected by their resource base (small invertebrates) and by predators (piscivorous fish and wading birds) (DeAngelis et al. 2005). In the seasonally fluctuating wetland, the effective resource base in the Everglades is positively related to flooded landscape area which varies tremendously with changes in water level. During the wet season the area available for small fishes to invade and exploit increases, while in the dry season the small fishes may be compressed into small areas of permanent water where density dependence and predation become important factors in their survival (Rehage and Trexler 2006).

In the Everglades, the small fishes move from permanently waterbodies (sloughs and canals) into wetlands as they re-flood, and their populations and biomass grow in size over the time span of the re-flooding. During the dry season, small fishes either retreat before the drying front or become trapped in shallow depressions where they are easily consumed by wading birds and other predators. The small fishes are able to track the flooding front, at movement rates approximating the velocity of the front, and expand in population size to produce much of the new biomass during the wet season (Gawlik 2002). It is very important to understand how small fishes disperse from discrete sources of permanent water throughout the newly opened area to build up biomass. Three types of movement are commonly identified for dispersal by animals: passive movements (such as with water currents), random active movements, and directed movements (Armsworth and Roughgarden 2005). In interior wetlands of the Everglades, water currents are low and passive dispersal seems too small to be considered. For dispersal involving active movements, it is usually assumed that the movements of individuals are random and that the spread of the population occurs through a combination of rete sources of permanent water throughout the newly opened arpopulation growth and random movements (Andow et al. 1990). Such a mechanism is described by a reaction–diffusion model (Fisher 1937; Skellam 1951) which predicts that invaders can form a traveling wave moving with an invasion speed depending on the intrinsic growth rate and the diffusion coefficient of the population (Aronson and Weinberger 1975; Okubo and Levin 2001).

An alternative mechanism is that individual fish movement is biased in the direction of the flooding front. Small invertebrates are most abundant at the edge of the moving front since rising water flushes out new resources that have not been exposed to exploitation by fish. The dynamic ideal free distribution hypothesis describes such a directed movement modeling approach and has recently been developed mathematically and applied in different contexts (Cosner 2005). Finally, the refuge mechanism demonstrates that there are small ponds and solution holes connected to the refugia which can maintain tiny populations of small fishes across the landscape during the dry season (Loftus et al. 1992). When water levels gradually rise again along an elevation gradient, the small fishes in these refugia would grow as soon as an area is flooded and might quickly fill up newly flooded areas. Gaff et al. (2000, 2004) noted

the possible importance of such refugia for Everglades fishes. To examine these three hypothesized mechanisms for their effectiveness in facilitating the spread and biomass growth of fishes filling the seasonally flooded area to carrying capacity, [DeAngelis et al. \(2010\)](#) modeled the growth and spread of small fishes on an idealized segment of marsh during the re-flooding phase and concluded that although refugia may play an important role in recolonization by the fish population during re-flooding, only taxis in the direction of the flooding front seems capable of matching empirical observations.

The regular pattern formation in real ecosystems has received a lot of attention from both ecologists and mathematicians. Turing's profound idea of regular pattern formation in chemical systems ([Turing 1952](#)), the so-called activator-inhibitor principle, is widely applied in analyzing physical systems as well as ecosystems ([Koch and Meinhardt 1994](#); [Murray 1993](#); [Ni and Tang 2005](#); [Okubo and Levin 2001](#)). This natural phenomenon can be found in many ecosystems such as mussel beds, air ecosystems, wetland ecosystems, savannas, coral reefs, ribbon forests, intertidal mudflats, and marsh tussocks ([Rietkerk and Koppel 2008](#)). The study of pattern formation in reaction–diffusion systems in wetland ecosystem is now active and important. Many wetland ecosystems undergo distinct wet and dry seasonal cycles. In the Florida Everglades ecosystem, a possible explanation for regular pattern formation in wetland is the nutrition redistribution through surface water flows generated by wet and dry seasonal cycle. There is increasing evidence linking regular pattern formation to scale-dependent feedback between organisms and their environment.

Fish biomass is a major energy resource in the Everglades ([DeAngelis et al. 2010](#)). The fish communities are influenced by fluctuations in water level in southern Florida ([Loftus and Kushlan 1987](#)). The high availability of nutrients in the system during flooding stimulates the rapid growth of microorganisms, invertebrates, and aquatic macrophytes, providing food and shelter for species that exploit this environment. In the Florida Everglades, small fishes are main food of wading birds. The environmental seasonality is reflected in patterns of fish biomass, which influence the food web of the ecosystem.

Our model assumes that the food chain consists of only small fish and their prey for simplicity. The prey is mainly invertebrates and they are the activator in Turing's principle. Unlike other fishes seasonal tropical wetlands and floodplains, no long-distance migrations of fishes as water recess in the Everglades was detected. However, as water rises, the surviving fishes of all size classes stream into recently re-flooded habitats. How far and how quickly water expand is important in the food web. In [Trexler et al. \(2001\)](#), it is hypothesized that the expansion re-flooding of marshes in the early wet season is often rapid as a result of dramatic rainfall. Thus, small fishes respond actively and they act as the inhibitor with faster diffusion rate.

The wet-dry seasonal cycle has the potential to limit the spatial scale of fish concentration during the water recession as well as expansion upon re-flooding. This mechanism gives rise to the scale-dependent feedback, which means the strength and sign of a feedback between organisms and their environment varies with distance. There are several movement types to model the diffusion of organisms. The passive dispersal such as water currents is not likely to occur in the Everglades since the re-flooding is mainly due to gradual rise of the underground water. Spatial explicit

reaction-advection-diffusion-type model is not likely to occur for the same reason. Since there is no long-distance migrations detected in the Everglades (Trexler et al. 2001), the movement of fish is assumed to be local and random. The reaction–diffusion model (Fisher 1937; Skellam 1951) described active movement like this and predicted possible mechanisms of spread.

The predator–prey system incorporated the Beddington–DeAngelis functional response (see Beddington 1975; DeAngelis et al. 1975) assumed that predators do not interference with the prey’s activities so the only competition occurs in the depletion of prey. Cantrell and Cosner (2001) investigated the permanence of the ODE model and the R-D system with no-flux boundary conditions. Hwang (2003, 2004) considered the global stability and the uniqueness of limit cycles in the ODE system. Yan and Zhang (2014) studied Turing instability and global stability of the positive constant steady state of the one-dimensional R-D system with homogeneous Neumann boundary conditions. Zhang et al. (2012) proposed to study the spatial dynamics of the Beddington–DeAngelis predator–prey model. They first transformed the ODE model with Beddington–DeAngelis functional response into a polynomial system by introducing a new time variable related to the original time by a nonlinear transformation involving the state variables. They then added spatial diffusion terms to the transformed (polynomial) system and studied the two-dimensional spatial patterns of the reaction–diffusion system thus obtained. In this paper, we add diffusion directly to the original predator–prey model with Beddington–DeAngelis functional response. This results in a reaction–diffusion system which is quite different from that considered by Zhang et al. (2012).

In this paper, we study the reaction–diffusion system by assuming that the movement of individuals is random. We also assume that there is no directed force in movement, which means that the system has very little underlying environmental heterogeneity. This is because passive movement, which is due to currents, is assumed to be too small in the Everglades. In other ecosystems, flooding is usually accompanied by water currents. However, in the Everglades, re-flooding is caused by gradual rise of underground water. The model takes the following form:

$$\begin{cases} \frac{\partial I(x,t)}{\partial t} = D_1 \Delta I(x,t) + r \left(1 - \frac{I(x,t)}{K}\right) I(x,t) - \frac{fI(x,t)F(x,t)}{1+hfI(x,t)+wfF(x,t)}, & x \in \Omega, \quad t > 0 \\ \frac{\partial F(x,t)}{\partial t} = D_2 \Delta F(x,t) + \frac{\gamma f I(x,t) F(x,t)}{1+hfI(x,t)+wfF(x,t)} - mF(x,t), & x \in \Omega, \quad t > 0, \end{cases} \tag{1}$$

where Ω represents the activate region for small fishes and their prey. Denote the small fish biomass density by variable $F(x,t)$ and invertebrate biomass by $I(x,t)$, where $x \in \Omega$ is the location, in units of kilometers, and $t > 0$ is time in days. The parameters D_2 and D_1 are diffusive coefficients of small fish and invertebrate, respectively, r is the growth rate of invertebrates, K is the invertebrate carrying capacity, f is the consumption coefficient, h is prey handling time, γ is the assimilation fraction, w is a predator interference coefficient, and m is the fish mortality rate. Predator consumption is described by the Beddington–DeAngelis functional response which is similar to Holling type II but has an extra term in the denominator.

For convenience, we make the nondimensionalized change of variables

$$t = rt, \quad u(x, t) = hfI(s, t), \quad v(x, t) = wfF(s, t), \quad D_1 = rd_1, \quad D_2 = rd_2, \quad (2)$$

$$k = khf, \quad f_1 = \frac{1}{wr}, \quad f_2 = \frac{\gamma}{rh}, \quad m = \frac{r-1}{r}m_1$$

and obtain the simplified dimensionless predator–prey system with Beddington–DeAngelis functional response:

$$\begin{cases} \frac{\partial u(x,t)}{\partial t} - d_1 \Delta u = \left(1 - \frac{u}{K}\right)u - \frac{f_1 uv}{1+u+v}, & x \in \Omega, \quad t > 0 \\ \frac{\partial v(x,t)}{\partial t} - d_2 \Delta v = \frac{f_2 uv}{1+u+v} - mv, & x \in \Omega, \quad t > 0. \end{cases} \quad (3)$$

where $x \in \Omega \subset R^n$ ($n = 1, 2$) is the spatial variable and $\Omega = \Omega_n \subset R^n$ ($n = 1, 2$) is the closed and bounded spatial domain which will produce one-dimensional and two-dimensional spatial Turing patterns. The parameters d_1 and d_2 are the scaled constant diffusion coefficients, $u(x, t)$ is the scaled invertebrate biomass density, and $v(x, t)$ is the scaled small fish biomass density.

Segel and Jackson (1972) was the first to show that Turing instability may occur in ecological systems; more precisely, they proved that the uniform steady state of a diffusive predator–prey model could be unstable if the predators exhibit self-limiting or intraspecific competition. Levin (1974) studied a similar model and obtained the same conclusion. Segel and Levin (1976) used a combination of successive approximation and multiple-time-scale theory to develop the small amplitude nonlinear theory for the diffusive predator–prey model considered in Segel and Jackson (1972) and showed that a new nonuniform steady state would be attained following destabilization of the spatially uniform steady state. Alonson et al. (2002) demonstrated that predator-dependent diffusive predator–prey models, such as the diffusive predator–prey model with ratio-dependent functional response function, can also generate patchiness in a homogeneous environment via Turing instability. Shi and Ruan (2015) studied the spatiotemporal patterns of a reaction-diffusion predator–prey system with mutual interference described by Crowley–Martin-type functional response, under homogeneous Neumann boundary conditions. Thus, the self-limiting or intraspecific competition effect of the predators can be relaxed if the predators exhibit mutual interference. For reviews and related work on Turing instability and Turing pattern formation of reaction–diffusion systems from applied sciences, we refer to Levin and Segel (1985), Murray (1993), and references cited therein.

The technique proposed in Segel and Levin (1976) to investigate the Turing patterns in predator–prey systems is now known as the *weakly nonlinear stability analysis*, which has been used to study the pattern formation aspects of convective stabilities in hydrodynamic morphological stabilities in solidification, and diffusive instabilities in ecology (Wollkind et al. 1994; Wollkind and Stephenson 2000), in particular the development of one- and two-dimensional Turing patterns in such systems. In this article, we study the stability and bifurcation of the positive steady state in both ODE and PDE models and give sufficient conditions for determining the Turing instability by linear analysis. For the reaction–diffusion systems, we prove the uniform boundedness and global stability under the Neumann boundary conditions. By weakly nonlinear analysis and singular perturbation theory, the asymptotic solutions of spatial Turing

patterns, including two-dimensional including rhombic and hexagonal patterns, are deduced.

2 Local Stability of the ODE System

In the section, we first consider the local stability of the following ordinary differential equations (Cantrell and Cosner 2001; Hwang 2003, 2004)

$$\begin{cases} \frac{du(t)}{dt} = u \left(1 - \frac{u}{K}\right) - \frac{f_1 uv}{1+u+v}, & t > 0 \\ \frac{dv(t)}{dt} = \frac{f_2 uv}{1+u+v} - mv, & t > 0. \end{cases} \tag{4}$$

For simplicity, denote

$$\begin{aligned} f(u, v) &= u \left(1 - \frac{u}{k}\right) - \frac{f_1 uv}{1+u+v}, \\ g(u, v) &= \frac{f_2 uv}{1+u+v} - mv. \end{aligned}$$

It is obvious that there are three equilibrium points:

$$E_1 = (0, 0), \quad E_2 = (k, 0), \quad E^* = (u^*, v^*)$$

where

$$u^* = \frac{\beta + \sqrt{\alpha}}{2f_2}, \quad v^* = \frac{(f_2 - m)u^* - m}{m}$$

with $\beta = k[f_2 - f_1(f_2 - m)]$, $\alpha = \beta^2 + 4mkf_2f_1$. The coexistence equilibrium [i.e., the constant steady state of the reaction–diffusion system (3)] (u^*, v^*) is in the first quadrant if and only if

$$(H_0) \quad f_2 > m, \quad u^* > \frac{m}{f_2 - m}.$$

From the viewpoint of ecology, the asymptotic properties of the positive equilibrium are interesting and important. For studying the local stability of the E^* , we consider the Jacobian matrix of the system (4) at E^* as following,

$$A := \begin{pmatrix} a_{11} & a_{12} \\ a_{21} & a_{22} \end{pmatrix}$$

where

$$\begin{aligned} a_{11} &= f_u(u^*, v^*) = -\frac{u^*}{k} + \frac{f_1 u^* v^*}{(1+u^*+v^*)^2} \\ a_{12} &= f_v(u^*, v^*) = -\frac{f_1 u^*}{1+u^*+v^*} + \frac{f_1 u^* v^*}{(1+u^*+v^*)^2} \\ a_{21} &= g_u(u^*, v^*) = \frac{f_2 v^*}{1+u^*+v^*} - \frac{f_2 u^* v^*}{(1+u^*+v^*)^2} \\ a_{22} &= g_v(u^*, v^*) = -\frac{f_2 u^* v^*}{(1+u^*+v^*)^2} \end{aligned}$$

For convenience, we set $\sigma = 1 - \frac{u^*}{k}$ and have

$$\begin{aligned} a_{11} &= \left(1 + \frac{m}{f_2}\right)\sigma - 1, & a_{12} &= \frac{m}{f_2}(\sigma - f_1), \\ a_{21} &= \frac{\sigma}{f_1}(f_2 - m), & a_{22} &= -\frac{m}{f_1}\sigma. \end{aligned}$$

We can see that

$$\operatorname{tr}(A) = a_{11} + a_{22} = \left(1 + \frac{m}{f_2} - \frac{m}{f_1}\right)\sigma - 1$$

and

$$\det(A) = a_{11}a_{22} + a_{12}a_{21} = \frac{m\sigma}{f_1} \left[-2\sigma + 1 + \frac{f_1}{f_2}(f_2 - m)\right].$$

It is well-known that the steady state E^* is locally asymptotically stable if $\operatorname{tr}(A) < 0$ and $\det(A) > 0$; and unstable if $\operatorname{tr}(A) > 0$. Thus, for the local stability of ODE system (1.4), we have the following theorem.

Theorem 2.1 *Assume (H_0) are satisfied,*

(i) *If*

$$(H_1) \quad \left(1 + \frac{m}{f_2} - \frac{m}{f_1}\right)\sigma < 1$$

and

$$(H_2) \quad 2\sigma < 1 + \frac{f_1}{f_2}(f_2 - m),$$

then the steady state E^ is locally asymptotically stable;*

(ii) *If*

$$(H_3) \quad \left(1 + \frac{m}{f_2} - \frac{m}{f_1}\right)\sigma > 1,$$

then the steady state E^ is unstable;*

(iii) *If*

$$(H_4) \quad 2\sigma > 1 + \frac{f_1}{f_2}(f_2 - m),$$

then the steady state E^ is a saddle point.*

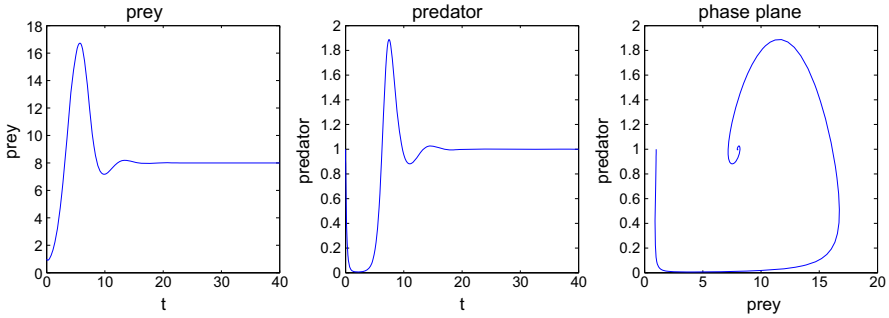


Fig. 1 (Color online) When $f_1 = 6, f_2 = 12, m = 9.6,$ and $k = 20,$ the positive equilibrium is asymptotically stable

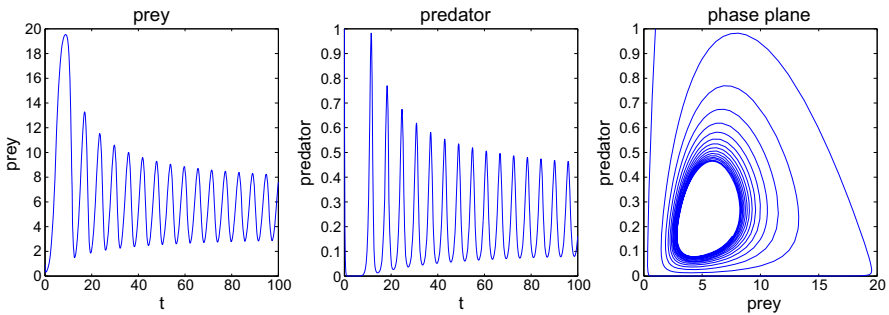


Fig. 2 (Color online) When $f_1 = 21, f_2 = 12, m = 9.6,$ and $k = 20,$ there is a limit cycle bifurcated from the positive equilibrium

In fact, if $a_{11} + a_{22} = (1 + \frac{m}{f_2} - \frac{m}{f_1})\sigma - 1$ changes from negative to zero and to positive when some parameter changes and the transversality condition is satisfied when the parameter takes the critical value, one can show that a Hopf bifurcation occurs at the positive steady state E^* when the parameter takes the critical value. Numerical simulations of the ODE model (4) with some parameter values are presented in Figs. 1 and 2. The positive equilibrium is asymptotically stable when $f_1 = 6, f_2 = 12, m = 9.6,$ and $k = 20$ (see Fig. 1). The positive equilibrium loses its stability, becomes unstable, and a periodic solution is bifurcated via Hopf bifurcation when $f_1 = 21, f_2 = 12, m = 9.6,$ and $k = 20$ (see Fig. 2).

3 Uniform Boundedness and Global Stability of the Reaction–Diffusion System

In this section, we first consider the dynamics of the diffusive predator–prey system

$$\begin{cases} \frac{\partial u(x,t)}{\partial t} - d_1 \Delta u = \left(1 - \frac{u}{k}\right)u - \frac{f_1 uv}{1+u+v}, & x \in \Omega, t > 0 \\ \frac{\partial v(x,t)}{\partial t} - d_2 \Delta v = \frac{f_2 uv}{1+u+v} - mv, & x \in \Omega, t > 0 \end{cases} \tag{5}$$

under the initial conditions

$$u(x, 0) = u_0(x), v(x, 0) = v_0(x) \tag{6}$$

and no-flux boundary conditions

$$\frac{\partial u}{\partial \nu} = \frac{\partial v}{\partial \nu} = 0, x \in \partial\Omega \tag{7}$$

where $\Omega \subset R^n$. Assume that the growth functions $f(u, v)$ and $g(u, v)$ are sufficiently smooth in R_+^2 . The standard partial differential equation theory shows that the solutions of (5) are unique and continuous for all positive times in Ω . The following theorem shows that the solutions of (5) are uniformly bounded.

Theorem 3.1 *Let $(u(x, t), v(x, t)) \in [C(\bar{\Omega} \times [0, T)) \cap C^{2,1}(\Omega \times (0, T))]$ ² be the solution of (5) with $u(x, 0) = u_0(x) \geq 0, v(x, 0) = v_0(x) \geq 0$. Then, $T = \infty$ and $0 \leq u(x, t) \leq M_1, 0 \leq v(x, t) \leq M_2$, where M_1, M_2 are defined as*

$$M_1 = \max \{ \| u_0 \|_\infty, k \}, M_2 = \max \left\{ \| v_0 \|_\infty, \frac{f_2 M_1}{m} \right\}.$$

Proof Since $0 \leq u(x, 0) \leq \| u_0 \|_\infty$ and

$$u_t - d_1 \Delta u \leq u \left(1 - \frac{u}{k} \right), (x, t) \in \Omega \times [0, \infty),$$

we have that $0 \leq u(x, t) \leq w(t)$ with $(x, t) \in \Omega \times [0, T)$, here $w(t) = [1/k + (1/ \| u_0 \|_\infty - 1/k)e^{-t}]^{-1}$ with $t \in [0, \infty)$ is the solution of the problem

$$\frac{dw(t)}{dt} = w \left(1 - \frac{w}{k} \right), w(0) = \| u_0 \|_\infty.$$

Hence, we have

$$0 \leq w(t) \leq \max \{ \| u_0 \|_\infty, k \}, t \in [0, \infty)$$

from the Theorem 2.1 in Shi and Ruan (2015). Thus,

$$0 \leq u(x, t) \leq w(t) \leq \max \{ \| u_0 \|_\infty, k \} \triangleq M_1$$

by the comparison argument of parabolic problems.

A similar argument holds for $v(x, t)$ satisfying

$$\begin{aligned} v_t - d_2 \Delta v &= v \left(\frac{f_2 u}{1+u+v} - m \right) = v \left(\frac{f_2 u - m(1+u) - mv}{1+u+v} \right) \\ &\leq v (f_2 u - mv) \leq v (f_2 M_1 - mv), \end{aligned}$$

the comparison argument shows that

$$0 \leq v(x, t) \leq \max \left\{ \|v_0\|_\infty, \frac{f_2 M_1}{m} \right\} \triangleq M_2.$$

Since the bound is independent of T , the solution exists globally. □

For the global stability of the steady state E^* of the PDE, we have the following theorem.

Theorem 3.2 *Assume that $f_1 - \frac{1}{k} < 0$. Then the positive constant steady state E^* with respect to system (5)–(7) is globally asymptotically stable, in other words, E^* attracts every positive solution of (5).*

Proof Let $(u(x, t), v(x, t))$ be the unique positive solution of system (5). Using Theorem 3.1, there exists a constant M which dose not depend on $x \in \bar{\Omega}$ and $t \geq 0$. By Theorem A2 in [Brown et al. \(1981\)](#), one has

$$\|u(\cdot, t)\|_{C^{2,\alpha}(\bar{\Omega})} \leq M, \|v(\cdot, t)\|_{C^{2,\alpha}(\bar{\Omega})} \leq M, \forall t \geq 1. \tag{8}$$

Define a Lyapunov function

$$E(t) = \alpha \int_{\Omega} \left(u - u^* - u^* \log \frac{u}{u^*} \right) dx + \beta \int_{\Omega} \left(v - v^* - v^* \log \frac{v}{v^*} \right) dx,$$

where $\alpha > 0, \beta > 0$ are constants and will be determined. Noting that $E(t) \geq 0$ for all $t > 0$, we can compute with respect to system (5),

$$\begin{aligned} \frac{dE(t)}{dt} &= \int_{\Omega} \left[\alpha d_1 \left(\frac{u-u^*}{u} \right) \Delta u + \beta d_2 \left(\frac{v-v^*}{v} \right) \Delta v \right] dx \\ &\quad + \int_{\Omega} \left[\alpha (u - u^*) \bar{f}(u, v) + \beta (v - v^*) \bar{g}(u, v) \right] dx \\ &\triangleq E_1(t) + E_2(t), \end{aligned}$$

where

$$\bar{f}(u, v) = 1 - \frac{u}{k} - \frac{f_1 v}{1 + u + v}, \quad \bar{g}(u, v) = \frac{f_2 u}{1 + u + v} - m$$

with $\bar{f}(u^*, v^*) = 0, \bar{g}(u^*, v^*) = 0$ and

$$\begin{aligned} E_1(t) &= \int_{\Omega} \left[\alpha d_1 \left(\frac{u-u^*}{u} \right) \Delta u + \beta d_2 \left(\frac{v-v^*}{v} \right) \Delta v \right] dx \\ E_2(t) &= \int_{\Omega} \left[\alpha (u - u^*) \bar{f}(u, v) + \beta (v - v^*) \bar{g}(u, v) \right] dx \end{aligned}$$

After some computations, we have that

$$E_1(t) = - \int_{\Omega} \left[\alpha d_1 \frac{u^*}{u^2} |\nabla u|^2 + \beta d_2 \frac{v^*}{v^2} |\nabla v|^2 \right] dx \leq 0$$

and

$$\begin{aligned}
 E_2(t) &= \int_{\Omega} [\alpha(u - u^*)\bar{f}(u, v) + \beta(v - v^*)\bar{g}(u, v)] \, dx \\
 &= \int_{\Omega} [\alpha(u - u^*)(\bar{f}(u, v) - \bar{f}(u^*, v^*)) + \beta(v - v^*)(\bar{g}(u, v) - \bar{g}(u^*, v^*))] \, dx \\
 &= \int_{\Omega} \alpha \left[\left(-\frac{1}{k} + \frac{f_1 v^*}{C}\right)(u - u^*)^2 + \frac{f_1}{C}(1 + u^*)(u - u^*)(v^* - v) \right] \\
 &\quad + \beta \left[\frac{f_2}{C}(1 + v^*)(u - u^*)(v - v^*) - \frac{f_2 u^*}{C}(v - v^*)^2 \right] \, dx,
 \end{aligned}$$

where $C = (1 + u + v)(1 + u^* v^*)$. Taking $\alpha = \frac{1}{f_1(1+u^*)} > 0, \beta = \frac{1}{f_2(1+v^*)} > 0$, we have

$$\begin{aligned}
 E_2(t) &= \int_{\Omega} \left[-\alpha \left(\frac{1}{k} - \frac{f_1 v^*}{C} \right) (u - u^*)^2 - \beta \frac{f_2 u^*}{C} (v - v^*)^2 \right] \, dx \\
 &= \int_{\Omega} \left[-\alpha l_1 (u - u^*)^2 - \beta l_2 (v - v^*)^2 \right] \, dx,
 \end{aligned}$$

where $l_1 = \frac{1}{k} - \frac{f_1 v^*}{(1+u+v)(1+u^* v^*)}, l_2 = \frac{f_2 u^*}{(1+u+v)(1+u^* v^*)} > 0$. By assumption $\frac{1}{k} > f_1$, we have $l_1 \geq \frac{1}{k} - f_1 > 0$. Noting that $u^2 \leq M, v^2 \leq M$, we have

$$E'(t) = E_1(t) + E_2(t) \leq -\tilde{M} \int_{\Omega} (|\nabla u|^2 + |\nabla v|^2) \, dx,$$

where $\tilde{M} > 0$ is a constant. Hence, we can conclude that $(u(x, t), v(x, t)) \rightarrow (u^*, v^*)$ in $[L^\infty(\Omega)]^2$, i.e., the global asymptotic stability of E^* . □

4 Local Stability of the Reaction–Diffusion System

In this part, we first derive conditions on the local stability for the spatially homogeneous equilibrium E^* of the diffusive system (3). Here, we consider two special cases with the Neumann boundary conditions in a one-dimensional interval $\Omega_1 = (0, 1)$ and a two-dimensional region $\Omega_2 = (0, 1) \times (0, 1)$:

$$\begin{cases} \frac{\partial u}{\partial t} - d_1 \Delta u = u \left(1 - \frac{u}{k} \right) - \frac{f_1 uv}{1+u+v}, & x \in \Omega_i, t > 0, \\ \frac{\partial v}{\partial t} - d_2 \Delta v = \frac{f_2 uv}{1+u+v} - mv, & x \in \Omega_i, t > 0, \end{cases} \tag{9}$$

with initial conditions

$$u(x, 0) = u_0(x) \geq 0, v(x, 0) = v_0(x) \geq 0, x \in \Omega_i \quad (i = 1, 2) \tag{10}$$

and Neumann boundary conditions

$$\frac{\partial u}{\partial \nu} = \frac{\partial v}{\partial \nu} = 0, x \in \partial\Omega_i, t > 0 \quad (i = 1, 2). \tag{11}$$

Here, we have (i) $\Delta = \frac{\partial^2}{\partial x^2}$, $x \in \Omega_1$, in one-dimensional domain; and (ii) $\Delta = \frac{\partial^2}{\partial x^2} + \frac{\partial^2}{\partial y^2}$ and $x = (x, y) \in \Omega_2$ in the two-dimensional spatial domain. ν is the outlet normal of the boundary $\partial\Omega_i$. We restrict ourselves to the case of the spatial domain Ω_2 and consider the temporal stability of the uniform steady state E^* for the two-dimensional spatial model.

The linearized system of (9) at E^* has the form:

$$\begin{pmatrix} u_t \\ v_t \end{pmatrix} = L \begin{pmatrix} u \\ v \end{pmatrix} := D \begin{pmatrix} \Delta u \\ \Delta v \end{pmatrix} + A \begin{pmatrix} u \\ v \end{pmatrix}, \tag{12}$$

where A is the Jacobian matrix defined in Sect. 2 and $D = \text{diag}(d_1, d_2)$. L is a linear operator with domain $D_L = X_C := \mathbf{X} \oplus \mathbf{iX} = \mathbf{x} + \mathbf{iy} : \mathbf{x}, \mathbf{y} \in \mathbf{X}$, where

$$X := \left\{ (u, v) \in H^2[(0, 1) \times (0, 1)] \times H^2[(0, 1) \times (0, 1)] \mid \frac{\partial u}{\partial \nu} = 0, \frac{\partial v}{\partial \nu} = 0, \mathbf{x}, \mathbf{y} \in \partial\Omega \right\}.$$

To solve this system of reaction–diffusion equations subject to the boundary conditions (11), we first define $\omega(\mathbf{x}) = (\mathbf{u}(\mathbf{x}), \mathbf{v}(\mathbf{x}))$ to be the time-independent solution of the spatial eigenvalue problem defined by

$$\nabla^2 \omega + \mathbf{k}^2 \omega = \mathbf{0}, \quad (\nu \cdot \nabla) \omega = \mathbf{0} \quad \text{for } \mathbf{x} \in \partial\Omega_2, \tag{13}$$

where k is the eigenvalue. The eigenvalue $k = n\pi$ in the one-dimensional case and $k^2 = |\mathbf{k}|^2 = \pi^2(\mathbf{n}^2 + \mathbf{m}^2)$ (n, m are integer) in the two-dimensional case. From now on, we refer to k as the wave number, with finite domains there is a discrete set of possible wave numbers.

Let $\omega_{\mathbf{k}}(\mathbf{x})$ be the eigenfunction corresponding to the wave number k . Each $\omega_{\mathbf{k}}(\mathbf{x})$ satisfies the zero-flux boundary conditions. Because the problem (12) is linear, we now consider solutions $(u(x, t), v(x, t))$ of (12) in the form

$$\begin{pmatrix} u(x, t) \\ v(x, t) \end{pmatrix} = \sum_k \begin{pmatrix} A_k \\ B_k \end{pmatrix} e^{\lambda t} \omega_{\mathbf{k}}(\mathbf{x}) = \sum_{\mathbf{k}} \begin{pmatrix} A_{\mathbf{k}} \\ B_{\mathbf{k}} \end{pmatrix} e^{\lambda t + \mathbf{i}\mathbf{k} \cdot \mathbf{x}}, \tag{14}$$

where the constants A_k and B_k are determined by the initial conditions and λ is the eigenvalue which determines the temporal growth. Substituting this form into (11) with (14) and canceling $e^{\lambda t}$, we obtain, for each k , that

$$\lambda \omega_{\mathbf{k}} = \mathbf{A} \cdot \omega_{\mathbf{k}} + \mathbf{D} \cdot \nabla^2 \omega_{\mathbf{k}} = \mathbf{A} \cdot \omega_{\mathbf{k}} - \mathbf{D} \cdot \mathbf{k}^2 \omega_{\mathbf{k}}. \tag{15}$$

We require nontrivial solutions for $\omega_{\mathbf{k}}$ so the λ is determined by the characteristic equation

$$P(\lambda, k, \sigma) \equiv \lambda^2 - T_k \lambda + D_k = 0, \tag{16}$$

where

$$\begin{aligned}
 k^2 &= \pi^2 (n^2 + m^2), \quad n, m = 0, 1, 2 \dots \\
 T_k &= a_{11} + a_{22} - k^2(d_1 + d_2) \\
 D_k &= d_1 d_2 k^4 - (d_2 a_{11} + d_1 a_{22}) k^2 + |A|.
 \end{aligned}$$

For convenient, let $d = d_1/d_2$ be the ratio of diffusion coefficients. Then

$$\begin{aligned}
 T_k &= \left(1 + \frac{m}{f_2} - \frac{m}{f_1}\right) \sigma - 1 - k^2 (1 + d), \\
 D_k &= dk^4 - \left[\left(1 + \frac{m}{f_2}\right) \sigma - 1\right] d - \frac{m}{f_1} \sigma \Big] k^2 + \left(-\frac{m}{f_1} \sigma\right) \left[2\sigma - 1 - f_1 \left(1 - \frac{m}{f_2}\right)\right]
 \end{aligned}$$

with $k^2 = d_1 k^2$. The roots of (16) yield the dispersion relation

$$\lambda_{1,2}(k) = \frac{1}{2} \left[T_k \pm \sqrt{T_k^2 - 4D_k} \right].$$

Recall that in Sect. 2, to obtain the local stability of the steady state E^* for the ODE system, we required that condition (H_1) holds; that is,

$$a_{11} + a_{22} = \left(1 + \frac{m}{f_2} - \frac{m}{f_1}\right) \sigma - 1 < 0.$$

Notice that $a_{22} = -\frac{m}{f_1} \sigma < 0$, to have $a_{11} + a_{22} < 0$, there are two subcases:

$$(H_{11}) \quad a_{11} = \left(1 + \frac{m}{f_2}\right) \sigma - 1 < 0 \quad \left(\text{i.e., } \sigma < \frac{f_2}{m + f_2}\right);$$

(in this case we always have $a_{11} + a_{22} < 0$, i.e., (H_1) always holds) and

$$(H_{12}) \quad a_{11} = \left(1 + \frac{m}{f_2}\right) \sigma - 1 > 0.$$

Now, we consider the stability of the steady state E^* for the diffusive system under the conditions (H_{11}) and (H_{12}) , respectively.

If we assume that condition (H_{11}) holds, then $T_k < 0$ and $D_k > 0$ when (H_1) holds. Thus, we can conclude that $\text{Re}(\lambda_{1,2}(k)) < 0$ for all $k \geq 0$. Therefore, we have the following result.

Proposition 4.1 *Assume that (H_{11}) hold, then the unique positive constant steady state E^* of the diffusive prey–predator system (9)–(11) is locally asymptotically stable (Fig. 3).*

Proposition 4.1 indicates that if both $a_{11} < 0$ and $a_{22} < 0$ hold, then the steady state E^* of the diffusive system is always locally asymptotically stable and Turing instability will not occur. Now, to discuss the occurrence of Turing instability, we

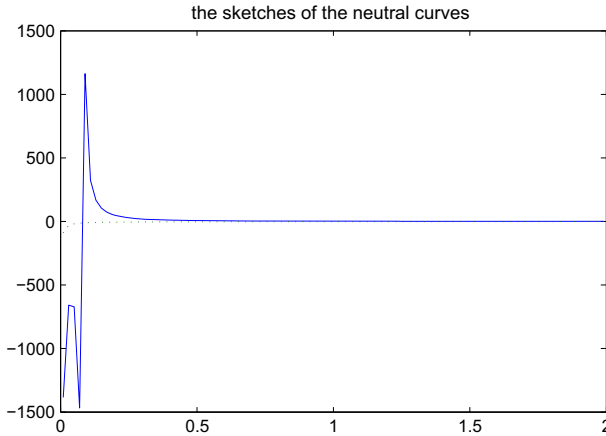


Fig. 3 (Color online) The behavior of the neutral curves L_1 and L_2 shows that the steady state is stable above the plane of curve L_2 and unstable under the plane. Here $f_1 = 6, f_2 = 12, m = 48/5, k = 20$

assume (H_1) along with (H_{12}) (that is, $a_{11} + a_{22} < 0$ but $a_{11} > 0$) and (H_2) (that is, $a_{11}a_{22} - a_{12}a_{21} > 0$) hold.

To obtain Turing instability, we first construct the neutral curves,

$$L_1 : T_k = \left(1 + \frac{m}{f_2} - \frac{m}{f_1}\right)\sigma - 1 - k^2(1 + d) = 0 \tag{17}$$

and

$$L_2 : D(k^2) := D_k = dk^4 - \left[\left(\left(1 + \frac{m}{f_2}\right)\sigma - 1\right)d - \frac{m}{f_1}\sigma\right]k^2 + \left(-\frac{m}{f_1}\sigma\right)\left[2\sigma - 1 - f_1\left(1 - \frac{m}{f_2}\right)\right] = 0 \tag{18}$$

It is necessary to determine the sign of $D(k^2)$. From (18), elementary differentiation with respect to k^2 implies that

$$\min_k D(k^2) = \left(-\frac{m}{f_1}\sigma\right)\left[2\sigma - 1 - f_1\left(1 - \frac{m}{f_2}\right)\right] - \frac{1}{4d}\left[\left(\left(1 + \frac{m}{f_2}\right)\sigma - 1\right)d - \frac{m}{f_1}\sigma\right]^2$$

at $k^2 = k_{min}^2$, where

$$k_{min}^2 = \frac{\left(\left(1 + \frac{m}{f_2}\right)\sigma - 1\right)d - \frac{m}{f_1}\sigma}{2d} > 0.$$

Let

$$\begin{aligned} \Pi(d) &:= \left[\left(\left(1 + \frac{m}{f_2} \right) \sigma - 1 \right) d - \frac{m}{f_1} \sigma \right]^2 \\ &\quad + 4d \left(\frac{m}{f_1} \sigma \right) \left[2\sigma - 1 - f_1 \left(1 - \frac{m}{f_2} \right) \right]. \end{aligned} \tag{19}$$

Then

$$\begin{aligned} \Pi(d) = 0 &\Leftrightarrow ad^2 + bd + c = 0, \\ \Theta(d) &:= \left(\left(1 + \frac{m}{f_2} \right) \sigma - 1 \right) d - \frac{m}{f_1} \sigma = 0 \Leftrightarrow d^* = \frac{\frac{m}{f_1} \sigma}{\left(1 + \frac{m}{f_2} \right) \sigma - 1}, \end{aligned}$$

where

$$\begin{aligned} a &= \left[\left(1 + \frac{m}{f_2} \right) \sigma - 1 \right]^2 > 0, \quad c = \left(\frac{m}{f_1} \sigma \right)^2 > 0, \\ b &= 2 \left(\frac{m}{f_1} \sigma \right) \left[(2\sigma - 1) - \frac{f_1}{f_2} (f_2 - m) - \left(1 - \frac{m}{f_2} \right) (f_1 - \sigma) \right] < 0. \end{aligned}$$

By computing, we obtain that $\Pi(d) = 0$ has two positive real roots,

$$d^+ = \frac{-b + \sqrt{\Delta_1}}{2a}, \quad d^- = \frac{-b - \sqrt{\Delta_1}}{2a},$$

where $\Delta_1 = 16 \left(\frac{m}{f_1} \sigma \right)^2 \left[(2\sigma - 1) - \frac{f_1}{f_2} (f_2 - m) \right] \left[\left(1 - \frac{m}{f_2} \right) (\sigma - f_1) \right] > 0$. We can see that $0 < d^- < d^* < d^+$ and $\min_k d(k^2) < 0, \Theta(d) > 0$ when $d > d^+$. Thus, the steady state E^* is unstable. This indicates that the Turing instability occurs.

Based on the above argument, we have the following theorem about Turing instability.

Theorem 4.2 *Assume that (H_1) , (H_{12}) , and (H_2) hold, then there exists an unbounded interval,*

$$I := \{d > 1 : d \geq d^+\}$$

for $d^+ > 0$, such that for any $d \in I$, the steady state E^* of the diffusive predator–prey system is unstable, that is, Turing instability occurs.

Remark 4.3 The conclusion of Theorem 4.2 also holds in the one-dimensional spatial reaction–diffusion system. Note that in the classical diffusive predator–prey model with Holling type II functional response, Turing instability does not occur unless the predators have a nonlinear death rate.

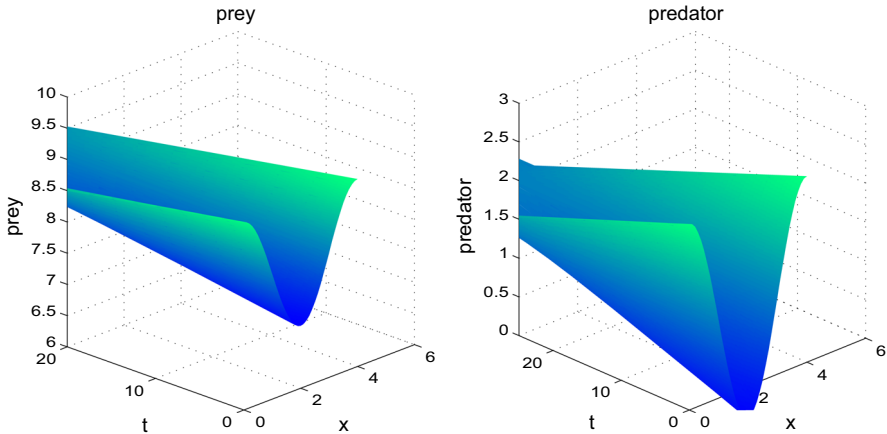


Fig. 4 (Color online) $f_1 = 6, f_2 = 12, m = 9.6, k = 20, d = 90,000$. The positive equilibrium of the diffusive system (20) is unstable

Example 4.4 As an example, we consider the following system:

$$\begin{cases} \frac{\partial u}{\partial t} - d_1 \Delta u = u \left(1 - \frac{u}{20}\right) - \frac{6uv}{1+u+v}, & x \in \Omega_i, t > 0, \\ \frac{\partial v}{\partial t} - d_2 \Delta v = \frac{12uv}{1+u+v} - \frac{48}{5}v, & x \in \Omega_i, t > 0, \end{cases} \tag{20}$$

where $d_1 = 1$ and $d_2 = 90000 > d^+$. The equilibrium $E^* = (8, 1)$ of the ODE model is stable (as shown in Fig. 1). However, E^* of the reaction–diffusion system is unstable, see Fig. 4.

5 Turing Patterns of the Reaction–Diffusion Systems

In this section, we consider the one-dimensional spatial patterns near the steady state E^* to the one-dimensional reaction–diffusion system and two-dimensional spatial patterns to the two-dimensional reaction–diffusion system by using the weakly nonlinear stability analysis technique introduced in Segel and Levin (1976) and Wollkind and Stephenson (2000). Consider the reaction–diffusion system

$$\begin{cases} \frac{\partial u}{\partial t} - d_1 \Delta u = u \left(1 - \frac{u}{k}\right) - \frac{f_1 uv}{1+u+v}, & x \in \Omega_i, t > 0, \\ \frac{\partial v}{\partial t} - d_2 \Delta v = \frac{f_2 uv}{1+u+v} - mv, & x \in \Omega_i, t > 0, \end{cases} \tag{21}$$

with initial conditions

$$u(x, 0) = u_0(x) \geq 0, v(x, 0) = v_0(x) \geq 0, \quad x \in \Omega_i, \tag{22}$$

and zero-flux boundary conditions

$$\frac{\partial u}{\partial \nu} = \frac{\partial v}{\partial \nu} = 0 \quad x \in \partial\Omega, t > 0. \tag{23}$$

As we have already seen, pattern formation may arise through Turing instability for certain ranges of parameter values. A necessary condition for this to occur is that the minimum of the neutral curve L_2 is less than zero, which yields the condition $d \geq d^+$.

We provide an approximating solution to (21) subject to initial conditions of the type

$$\begin{pmatrix} u(x, 0) \\ v(x, 0) \end{pmatrix} = \varepsilon \begin{pmatrix} u_0(x) \\ v_0(x) \end{pmatrix}, \tag{24}$$

where ε is a small parameter that will be seen to be related to $d - d_c$, and

$$d_c = \frac{[(m/f_1)\sigma][k_c^2 + 1 + f_1(f_2 - m)/f_2 - 2\sigma]}{[k_c^2(k_c^2 + 1 - (f_2 + m)\sigma/f_2)]} \quad (d_c > d^+) \tag{25}$$

is given on the neutral curve L_2 .

To find solutions which are $o(\varepsilon)$ uniformly in time, we set up the successive approximation procedure

$$\begin{pmatrix} u - u^* \\ v - v^* \end{pmatrix} \sim \varepsilon \begin{pmatrix} u_1 \\ v_1 \end{pmatrix} + \varepsilon^2 \begin{pmatrix} u_2 \\ v_2 \end{pmatrix} + \varepsilon^3 \begin{pmatrix} u_3 \\ v_3 \end{pmatrix}. \tag{26}$$

Since we consider the Turing spatial solutions at $o(\varepsilon)$, it is natural to expand the reaction dynamics functions $f(u, v)$ and $g(u, v)$ at E^* . Substituting (26) into (21)–(23), we obtain the recursive series of equations,

$$\begin{pmatrix} \frac{\partial u_n}{\partial t} \\ \frac{\partial v_n}{\partial t} \end{pmatrix} = D \begin{pmatrix} \Delta u_n \\ \Delta v_n \end{pmatrix} + A_c \begin{pmatrix} u_n \\ v_n \end{pmatrix} + N(u_{n-1}, v_{n-1}, \sigma), \tag{27}$$

where $D = \text{diag}(1, d)$ and A_c is given in the linear theory,

$$A_c = \begin{pmatrix} \theta_1 & -\theta_2 \\ \theta_3 & -\theta_4 \end{pmatrix}$$

with

$$\begin{aligned} \theta_1 &= \left[\left(1 + \frac{m}{f_2} \right) \sigma - 1 \right], & \theta_2 &= \frac{m}{f_2} (f_1 - \sigma), \\ \theta_3 &= \frac{\sigma}{f_1} (f_2 - m), & \theta_4 &= \frac{m}{f_1} \sigma \end{aligned}$$

and

$$N(u, v, \sigma) = \begin{pmatrix} F(u, v, \sigma) \\ G(u, v, \sigma) \end{pmatrix} = \begin{pmatrix} -\frac{1}{k} \\ 0 \end{pmatrix} u^2 + \begin{pmatrix} -f_1 \\ f_2 \end{pmatrix} (s_1 u^2 - s_3 uv + s_2 v^2) + \dots,$$

where

$$s_1 = \left(\frac{1}{f_1}\right) \left(\frac{m}{f_2}\right) \left(1 - \frac{m}{f_2}\right) \frac{\sigma}{k(1-\sigma)}, \quad s_2 = \left(\frac{m}{f_2}\right)^2 \frac{f_1 - \sigma}{k(1-\sigma)},$$

$$s_3 = \left(\frac{m}{f_2}\right)^2 \frac{f_1 + 2k\sigma(1-\sigma)}{k^2(1-\sigma)^2}.$$

5.1 One-Dimensional Patterns of One-Dimensional Reaction–Diffusion Systems

In order to investigate the occurrence of one-dimensional patterns in model (21), we begin our discussion by putting

$$d = d_c - \bar{d}\varepsilon^2, \tag{28}$$

where $0 < \varepsilon \ll 1$ is a small parameter, \bar{d} is of $o(1)$, depending on whether the pattern form bifurcates initially into d_c , which is given by (25) for some k . The local stability of the pattern solutions may be determined by introducing the slow time scale $\tau = \varepsilon^2 t$ with

$$\frac{\partial}{\partial t} = \frac{\partial}{\partial t} + \varepsilon^2 \frac{\partial}{\partial \tau}. \tag{29}$$

Substituting (28)–(29) into (27), we obtain that the leading term (u_1, v_1) satisfying the following equations at $o(\varepsilon)$

$$L_c[u_1, v_1]^T = 0 \tag{30}$$

with zero-flux boundary conditions, where the operator L_c is given by

$$L_c = \begin{bmatrix} \frac{\partial}{\partial t} - d_1 \frac{\partial^2}{\partial x^2} - \theta_1 & \theta_2 \\ -\theta_3 & \frac{\partial}{\partial t} - d_c d_1 \frac{\partial^2}{\partial x^2} + \theta_4 \end{bmatrix}.$$

Now, we consider a solution of the leading term (u_1, v_1) of the form

$$\begin{pmatrix} u_1 \\ v_1 \end{pmatrix} = \begin{pmatrix} A_1 \\ A_2 \end{pmatrix} e^{\lambda t} \cos(q_c x). \tag{31}$$

Here, $q_c = k_c/\sqrt{d_1} = \pi k/\sqrt{d_1}$ (k is an integer) is the critical wave number of the local linear stability theory, and the amplitude A_i ($i = 1, 2$) is the function of the slow time scale τ . By the local linear stability in Sect. 4, we obtain the amplitude A_i satisfying

$$M_c \begin{pmatrix} A_1 \\ A_2 \end{pmatrix} = \lambda_0 \begin{pmatrix} A_1 \\ A_2 \end{pmatrix}, \tag{32}$$

where M_c is the linearization matrix

$$M_c = \begin{pmatrix} \theta_1 - q_c^2 & -\theta_2 \\ \theta_3 & -\theta_4 - d_c q_c^2 \end{pmatrix}.$$

To obtain the nonzero solution of the leading term (u_1, v_1) , we let

$$F_c(\lambda_0, q_c, d_c) := \det(\lambda_0 I - M_c) = (\lambda_0 + q_c^2 - \theta_1)(\lambda_0 + d_c q_c^2 + \theta_4) + \theta_2 \theta_3 \tag{33}$$

and require that $F_c = 0$. By the local stability analysis in Sect. 4, we obtain that $\lambda_0 = 0$ or $\lambda_0 = T_k < 0$ when d_c is on the neutral curve L_2 . Without loss of generality, the leading term is assumed to be given by some initial conditions,

$$\begin{pmatrix} u_1 \\ v_1 \end{pmatrix} = A(\tau) \begin{pmatrix} A_1 \\ A_2 \end{pmatrix} \cos(q_c x), \quad \lambda_0 = 0, \tag{34}$$

where $A_1/A_2 = [\theta_4 + d_c q_c^2]/\theta_3$. At $o(\varepsilon^2)$, the equations of (u_2, v_2) satisfy

$$L_c \begin{pmatrix} u_2 \\ v_2 \end{pmatrix} = \begin{pmatrix} -\frac{1}{k} \\ 0 \end{pmatrix} u_1^2 + \begin{pmatrix} f_1 \\ -f_2 \end{pmatrix} (s_1 u_1^2 - s_3 u_1 v_1 + s_2 v_1^2). \tag{35}$$

We consider only the particular integral part of the general solution of (35), since the homogenous part (about $\cos(q_c x)$) can be absorbed into the leading order term by suitable modification of A . The appropriate solution of Eq. (35) can be written, after some algebra, as

$$\begin{pmatrix} u_2 \\ v_2 \end{pmatrix} = A^2(\tau) \left[\begin{pmatrix} p_{11} \\ p_{21} \end{pmatrix} \cos(2q_c x) + \begin{pmatrix} p_{12} \\ p_{22} \end{pmatrix} \right],$$

where

$$p_{11} = \frac{Q_1(2q_c)}{F(0, 2q_c, d_c)}, \quad p_{21} = \frac{Q_2(2q_c)}{F(0, 2q_c, d_c)},$$

$$p_{12} = \frac{Q_1(0)}{F(0, 0, d_c)}, \quad p_{22} = \frac{Q_2(0)}{F(0, 0, d_c)},$$

with

$$p = s_1 A_1^2 - 2s_3 A_1 A_2 + s_2 A_2^2,$$

$$Q_1(q_c) = \frac{A_1^2}{f_{1k}} (m\sigma - f_1 d_c q_c^2) - f_1 p (m - d_c q_c^2), \tag{36}$$

$$Q_2(q_c) = \frac{A_1^2}{f_{1k}} (f_2 - m)\sigma - f_2 p (2\sigma - 1 - q_c^2).$$

At $o(\varepsilon^3)$, the equations determining (u_3, v_3) become

$$L_c \begin{pmatrix} u_3 \\ v_3 \end{pmatrix} = - \begin{pmatrix} \frac{\partial u_1}{\partial \tau} \\ \frac{\partial v_1}{\partial \tau} \end{pmatrix} + \begin{pmatrix} 0 \\ \bar{d}\nabla^2 v_1 \end{pmatrix} + \begin{pmatrix} -\frac{1}{k} \\ 0 \end{pmatrix} 2u_1u_2 + \begin{pmatrix} f_1 \\ -f_2 \end{pmatrix} 2[s_1u_1u_2 - s_3(u_1v_2 + u_2v_1) + s_2v_1v_2]. \tag{37}$$

The resonant forcing function is shown in the left-hand side of Eq. (37). The solution is only possibly satisfied by providing the Fredholm solvability condition which determines the amplitude A on the slow time scale τ . After some long algebra, we find that the solvability condition requires that (Fig. 5)

$$E \frac{dA}{d\tau} = \delta A - DA^3, \tag{38}$$

which is also called the amplitude equation, where $E = \theta_3 + (\theta_4 + d_cq_c^2)A_2/A_1 > 0$, $\delta = \bar{d}q_c^2(d_cq_c^2 + \theta_4)$, and D is the Landau constant given by

$$D = \frac{1}{k}\theta_3 \left(\frac{1}{2}p_{11} + p_{12}\right) + [f_1\theta_3 - f_2(\theta_4 + d_cq_c^2)] [(p_{11} + 2p_{12})(s_1 - s_3A_2/A_1) + (p_{21} + 2p_{22})(s_2A_2/A_1 - s_3)]. \tag{39}$$

Now, we consider the critical points of the amplitude equation:

$$(a)A_0 = 0, \quad (b)A_0^2 = \frac{\delta}{D},$$

which yield the stability criteria that (a) is stable for $\delta < 0$ and unstable for $\delta > 0$; (b) is stable for $\delta > 0$ and unstable for $\delta < 0$.

Since we need to consider the nonzero critical point of the amplitude equation (38), we close this section with an interpretation of the potential stability about the critical point (b). It is clearly that the critical point (b) is unstable with $D < 0$ when $\delta < 0$ (i.e., $d < d_c$) and stable with $D > 0$ for $\delta > 0$ (i.e., $d > d_c$). Then, the lowest order solution, which is relative to the Turing pattern, is given by the critical point (b) as follows

$$\begin{pmatrix} u \\ v \end{pmatrix} \sim \begin{pmatrix} u^* \\ v^* \end{pmatrix} + \sqrt{\frac{\delta}{D}} \begin{pmatrix} A_1 \\ A_2 \end{pmatrix} \cos(q_c x),$$

where the Landau constant D is given by (39). We can examine the sign of the Landau constant D and plot the patterns for given parameters.

5.2 Rhombic Patterns of Two-Dimensional Reaction–Diffusion Systems

As in the one-dimensional analysis, set

$$d = d_c - \bar{d}\varepsilon^2, \tag{40}$$

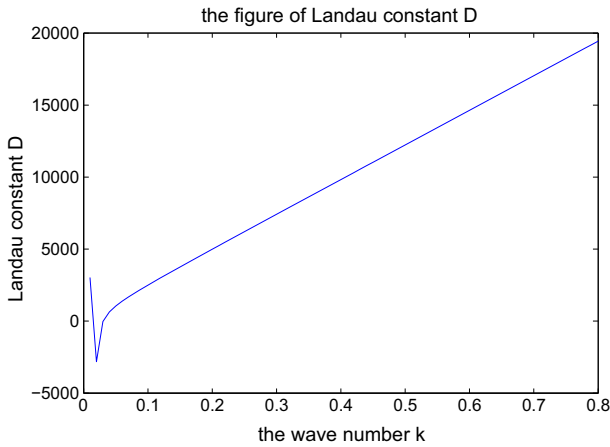


Fig. 5 (Color online) The behavior of the Landau constant D . The stable spatial patterns appear at the points where $D > 0$. Here $f_1 = 6$, $f_2 = 12$, $m = 48/5$, $k = 20$

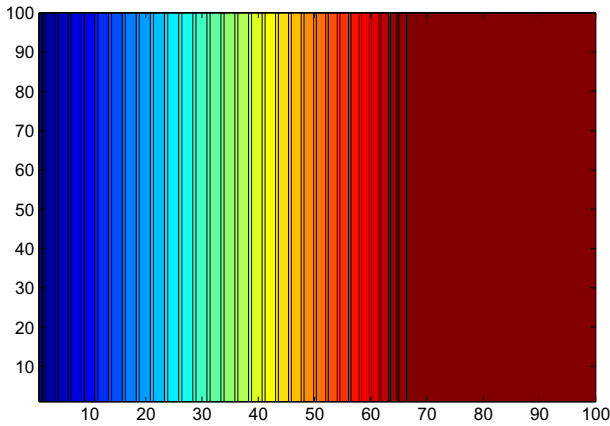


Fig. 6 (Color online) The one-dimensional stable spatial pattern

where d_c is given in (25) with $k_c^2 = d_1\pi(n^2 + m^2)$ being the critical wave number, and introduce the slow time scale (Fig. 6),

$$\frac{\partial}{\partial t} = \frac{\partial}{\partial t} + \varepsilon^2 \frac{\partial}{\partial \tau}. \tag{41}$$

In order to study the spatial rhombic patterns in the two-dimensional system, we consider a solution of the leading term (u_1, v_1) of the form under the corresponding initial conditions,

$$\begin{pmatrix} u_1 \\ v_1 \end{pmatrix} = \begin{pmatrix} A_1 \\ A_2 \end{pmatrix} e^{\lambda t} \cos(q_c x) + \begin{pmatrix} B_1 \\ B_2 \end{pmatrix} e^{\lambda t} \cos(q_c z), \tag{42}$$

where $z = \cos(\psi)x + \sin(\psi)y$, ψ is the characteristic angle of a rhombic pattern, $q_c = d_1 k_c$. Substituting (40)–(42) into (27), we obtain the leading term satisfying

$$\tilde{L}_c[u_1, v_1]^+ = 0,$$

where

$$\tilde{L}_c = \begin{bmatrix} \frac{\partial}{\partial t} - d_1 \left(\frac{\partial^2}{\partial x^2} + \frac{\partial^2}{\partial y^2} \right) - \theta_1 & \theta_2 \\ -\theta_3 & \frac{\partial}{\partial t} - d_c d_1 \left(\frac{\partial^2}{\partial x^2} + \frac{\partial^2}{\partial y^2} \right) + \theta_4 \end{bmatrix}.$$

After some complicated algebraic computations, we obtain the spatial leading term under some fixed initial conditions,

$$\begin{pmatrix} u_1 \\ v_1 \end{pmatrix} = A(\tau) \begin{pmatrix} A_1 \\ A_2 \end{pmatrix} \cos(q_c x) + B(\tau) \begin{pmatrix} A_1 \\ A_2 \end{pmatrix} \cos(q_c z),$$

where $A_1/A_2 = [\theta_4 + d_c q_c^2]/\theta_3$. To continue, the solutions (u_2, v_2) at $o(\varepsilon^2)$ are most conveniently obtained after some computing,

$$\begin{pmatrix} u_2 \\ v_2 \end{pmatrix} = \begin{pmatrix} p_{11} \\ p_{21} \end{pmatrix} [A^2 \cos(2q_c x) + B^2 \cos(2q_c z)] + \begin{pmatrix} p_{12} \\ p_{22} \end{pmatrix} AB \cos[q_c(x + z)] \\ + \begin{pmatrix} p_{13} \\ p_{23} \end{pmatrix} AB \cos[q_c(x - z)] + \begin{pmatrix} p_{14} \\ p_{24} \end{pmatrix} [A^2 + B^2],$$

where

$$p_{11} = \frac{Q_1(2q_c)}{F(0, 2q_c, d_c)}, \quad p_{12} = \frac{Q_1(\sqrt{2+2\cos\psi}q_c)}{F(0, \sqrt{2+2\cos\psi}q_c, d_c)}, \quad p_{13} = \frac{Q_1(\sqrt{2-2\cos\psi}q_c)}{F(0, \sqrt{2-2\cos\psi}q_c, d_c)}, \quad p_{14} = \frac{Q_1(0)}{F(0, 0, d_c)}, \\ p_{21} = \frac{Q_2(2q_c)}{F(0, 2q_c, d_c)}, \quad p_{22} = \frac{Q_2(\sqrt{2+2\cos\psi}q_c)}{F(0, \sqrt{2+2\cos\psi}q_c, d_c)}, \quad p_{23} = \frac{Q_2(\sqrt{2-2\cos\psi}q_c)}{F(0, \sqrt{2-2\cos\psi}q_c, d_c)}, \quad p_{24} = \frac{Q_2(0)}{F(0, 0, d_c)}$$

and p, Q_1, Q_2 are given in (36), the function F is given in (33). At $o(\varepsilon^3)$, the equations of (u_3, v_3) become

$$\tilde{L}_c^1 \begin{pmatrix} u_3 \\ v_3 \end{pmatrix} = - \begin{pmatrix} \frac{\partial u_1}{\partial \tau} \\ \frac{\partial v_1}{\partial \tau} \end{pmatrix} + \begin{pmatrix} 0 \\ \bar{d}\nabla^2 v_1 \end{pmatrix} + \begin{pmatrix} -\frac{1}{k} \\ 0 \end{pmatrix} 2u_1 u_2 \\ + \begin{pmatrix} f_1 \\ -f_2 \end{pmatrix} 2[s_1 u_1 u_2 - s_3(u_1 v_2 + u_2 v_1) + s_2 v_1 v_2]. \tag{43}$$

Hence, we obtain equations of the amplitudes $A(\tau)$ and $B(\tau)$ by the solvability conditions

$$E \frac{dA}{d\tau} = \delta A - A(D_1 A^2 + D_2 B^2) \\ E \frac{dB}{d\tau} = \delta B - B(D_2 A^2 + D_1 B^2), \tag{44}$$

where $E > 0$ is a constant and $\delta = \bar{d}q_c^2(\theta_4 + q_c^2d_c)A_2/A_1$, D_1 and D_2 are Landau constants given by

$$\begin{aligned}
 D_1 &= \frac{\theta_3}{k} (p_{11} + 2p_{13}) + [\theta_3 f_1 - f_2 (\theta_4 + d_c q_c^2)] \\
 &\quad [(p_{11} + 2p_{13}) (s_1 - s_3 A_2/A_1) + ((p_{21} + 2p_{23}) (s_2 A_2/A_1 - s_3))], \\
 D_2 &= \frac{\theta_3}{k} (p_{11} + p_{12} + 2p_{13}) + [\theta_3 f_1 - f_2 (\theta_4 + d_c q_c^2)] \\
 &\quad [(p_{11} + p_{12} + 2p_{13}) (s_1 - s_3 A_2/A_1) + ((p_{21} + p_{22} + 2p_{23}) (s_2 A_2/A_1 - s_3))].
 \end{aligned}
 \tag{45}$$

We now turn our attention to the rhombic planform amplitude equations (44) which possess the following equivalent classes of critical points:

$$\begin{aligned}
 \text{(I)} \quad &A_0 = B_0 = 0, & \text{(II)} \quad &A_0^2 = \frac{\delta}{D_1}, B_0 = 0, \\
 \text{(III)} \quad &B_0^2 = \frac{\delta}{D_1}, A_0 = 0, & \text{(IV)} \quad &A_0^2 = B_0^2 = \frac{\delta}{D_1 + D_2}.
 \end{aligned}$$

Assuming that $D_1 > 0$, $D_1 + D_2 > 0$, and investigating the stability of the critical points by linearization theory, we first give the Jacobian matrix $J(A_0, B_0)$ as

$$J(A_0, B_0) = \begin{pmatrix} \delta - (3D_1 A^2 + D_2 B^2) & -2D_2 AB \\ -2D_2 AB & \delta - (3D_1 B^2 + D_2 A^2) \end{pmatrix}_{(A_0, B_0)}$$

and determine the eigenvalues λ as solutions of

$$|\lambda I - J(A_0, B_0)| = \begin{vmatrix} \lambda - \delta + (3D_1 A_0^2 + D_2 B_0^2) & 2D_2 A_0 B_0 \\ 2D_2 A_0 B_0 & \lambda - \delta + (3D_1 B_0^2 + D_2 A_0^2) \end{vmatrix} = 0$$

i.e.,

$$(\lambda - \delta)^2 + b(\lambda - \delta) + c = 0, \tag{46}$$

where $b = (3D_1 + D_2)(A_0^2 + B_0^2)$, $c = (3D_1 A_0^2 + D_2 B_0^2)(3D_1 B_0^2 + D_2 A_0^2) - 4D_2^2 A_0^2 B_0^2$. We find that λ has the associated roots with corresponding critical points,

$$\begin{aligned}
 \text{(I)} \quad &\lambda_{1,2} = \delta, \\
 \text{(II)(III)} \quad &\lambda_1 = -5\delta \quad \lambda_2 = \delta \left(1 - \frac{2D_2}{D_1}\right), \\
 \text{(IV)} \quad &\lambda_1 = -5\delta \quad \lambda_2 = \delta \frac{4D_2 - 5D_1}{D_1 + D_2}.
 \end{aligned}$$

Noticing that the stability of the critical points (I)–(IV) is determined by the sign of the characteristic roots $\lambda_i (i = 1, 2)$, we can obtain the stability criteria as follows: (I) is stable for $\delta > 0$; (II) is stable for $2D_2 > D_1, \delta > 0$ [(III) is the same as (II)]; and (IV) is stable for $4D_2 - 5D_1 < 0, \delta > 0$. The Landau constants D_1 and D_2 will be determined after the successive computing (Figs. 7, 8, 9, 10).

It is clear that the lowest spatial nonzero Turing solution associated with two critical points [(II), (IV)] is given by

$$\text{(II)} : \begin{pmatrix} u_1 \\ v_1 \end{pmatrix} \sim \begin{pmatrix} u^* \\ v^* \end{pmatrix} + \sqrt{\frac{\delta}{D_1}} \begin{pmatrix} A_1 \\ A_2 \end{pmatrix} \cos(q_c x) \tag{47}$$

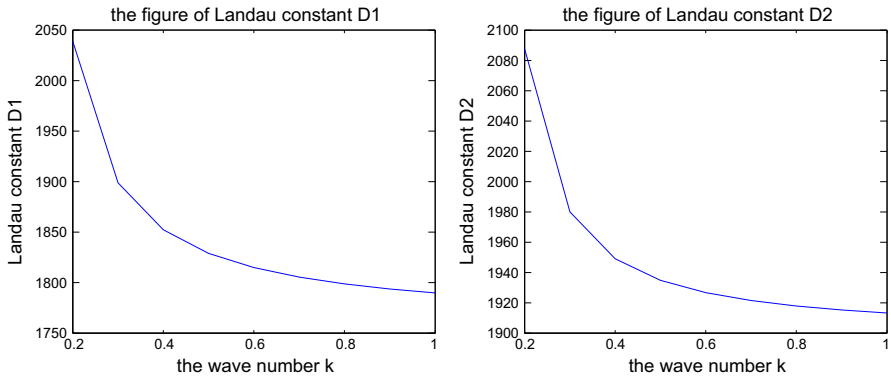


Fig. 7 (Color online) The plots of Landau constants D_1 and D_2 with the wave number q_c^2

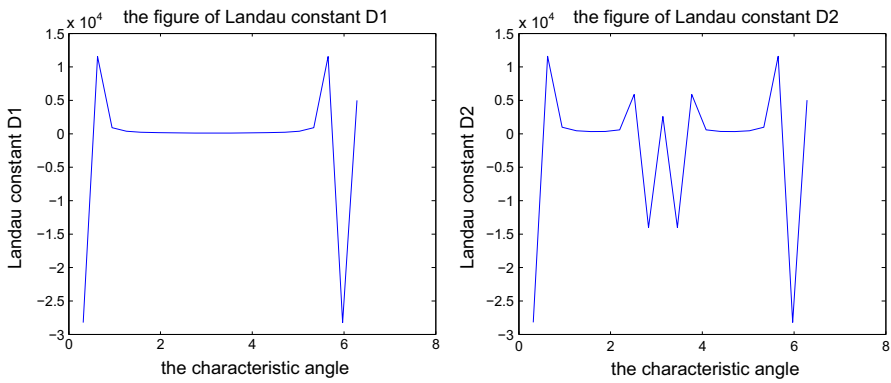


Fig. 8 (Color online) The plots of Landau constants D_1 and D_2 with the characteristic ψ

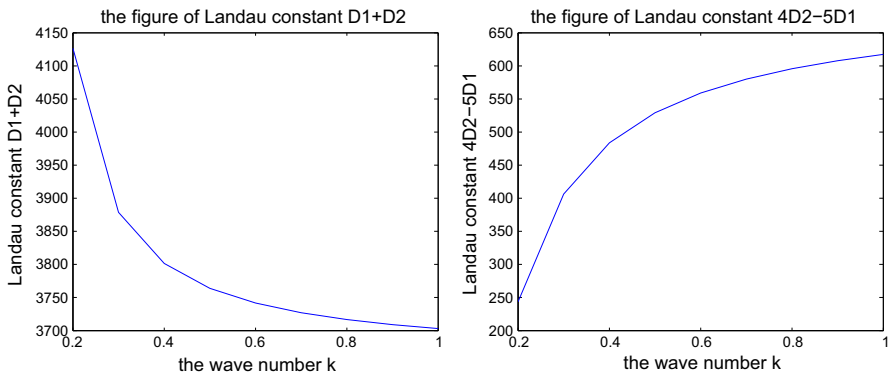


Fig. 9 (Color online) The sketches of Landau constants $D_1 + D_2$ and $4D_2 - 5D_1$ with the wave number q_c^2

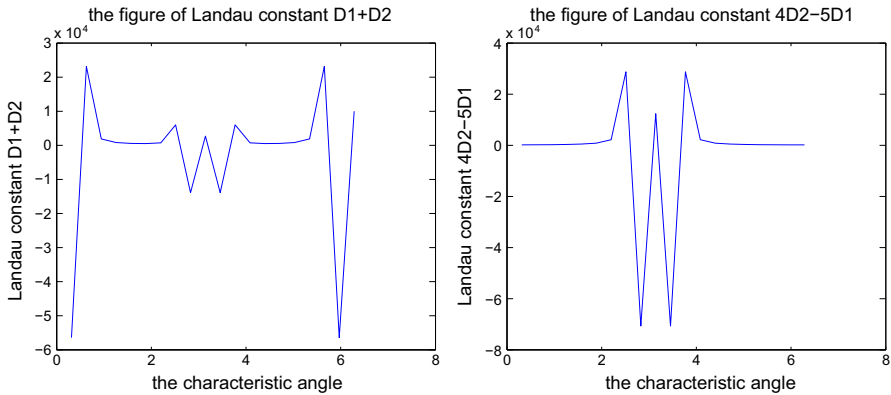


Fig. 10 (Color online) The sketches of Landau constants $D_1 + D_2$ and $4D_2 - D_1$ with the characteristic ψ

and

$$(IV) : \begin{pmatrix} u_1 \\ v_1 \end{pmatrix} \sim \begin{pmatrix} u^* \\ v^* \end{pmatrix} + \sqrt{\frac{\delta}{D_1 + D_2}} \begin{pmatrix} A_1 \\ A_2 \end{pmatrix} [\cos(q_c x) + \cos(q_c z)]. \quad (48)$$

Note that (II), as in one-dimensional analysis, represents the homogeneous and striped state patterns, while (IV) is identified with a rhombic pattern possessing characteristic angle ψ in [Wollkind and Stephenson \(2000\)](#). To demonstrate the rhombic pattern, we obtain the pattern solutions at $o(\varepsilon)$ in the form

$$\begin{aligned} \begin{pmatrix} u - u^* \\ v - v^* \end{pmatrix} &\sim \sqrt{\frac{\delta}{D_1 + D_2}} \begin{pmatrix} A_1 \\ A_2 \end{pmatrix} [\cos(q_c x) + \cos(q_c z)] \\ &= \sqrt{\frac{\delta}{D_1 + D_2}} \begin{pmatrix} A_1 \\ A_2 \end{pmatrix} \cos \omega_1 \cos \omega_2, \end{aligned} \quad (49)$$

where $\omega_1 = q_c(x + z) = q_c[(1 + \cos \psi)x + (\sin \psi)y]$ and $\omega_2 = q_c(x - z) = q_c[(1 - \cos \psi)x - (\sin \psi)y]$. From ω_1 and ω_2 , we can deduce that the intersecting level curves in the associated contour plot are two families of straight lines possessing slopes of $K_1 = -[1 + \cos \psi]/\sin \psi$ and $K_2 = [1 - \cos \psi]/\sin \psi$ with $K_1 K_2 = -1$. Therefore, we can give such a leading spatial solution as Turing pattern of a rhombic array of rectangles in (49) (Figs. 11, 12).

5.3 Hexagonal Planform Patterns of the Reaction–Diffusion Systems

In order to investigate the occurrence of hexagonal patterns, we consider a solution of the leading term (u_1, v_1) of the form

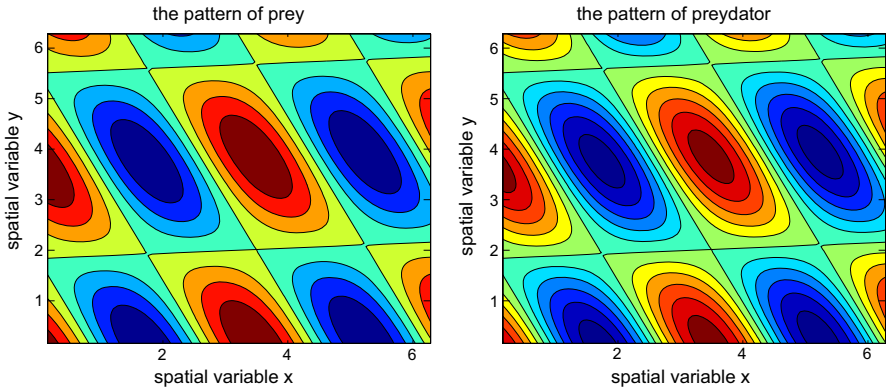


Fig. 11 (Color online) The two-dimensional stable rhombic patterns with $q_c^2 = 0.4$, $\psi = \pi/5$

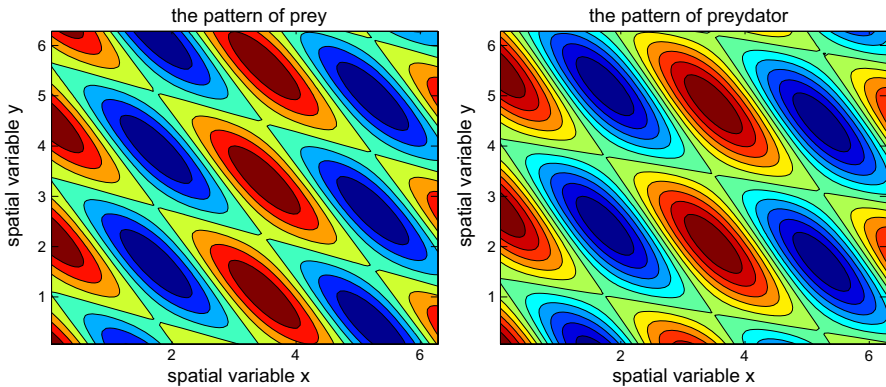


Fig. 12 (Color online) The two-dimensional stable rhombic patterns with $q_c^2 = 0.4$, $\psi = \pi/20$

$$\begin{aligned} \begin{pmatrix} u_1 \\ v_1 \end{pmatrix} &= \begin{pmatrix} A_1 \\ A_2 \end{pmatrix} e^{\lambda t} \cos(q_c x) + \begin{pmatrix} A_3 \\ A_4 \end{pmatrix} e^{\lambda t} \cos\left(q_c \frac{x - \sqrt{3}y}{2}\right) \\ &+ \begin{pmatrix} A_5 \\ A_6 \end{pmatrix} e^{\lambda t} \cos\left(q_c \frac{x + \sqrt{3}y}{2}\right). \end{aligned} \tag{50}$$

Similarly, we consider the bifurcation parameter d , and the time derivatives are accordingly replaced using

$$d = d_c - d_0 \varepsilon - \bar{d} \varepsilon^2 \tag{51}$$

and

$$\frac{\partial}{\partial t} = \frac{\partial}{\partial t} + \varepsilon \frac{\partial}{\partial \tau_1} + \varepsilon^2 \frac{\partial}{\partial \tau_2}, \tag{52}$$

where d_c is given by (25), d_0 and \bar{d} are the $o(\varepsilon)$ and $o(\varepsilon^2)$ scales, respectively, τ_1 and τ_2 are the slow time scales in the amplitude. By successive computing, we first give the spatial solution of the leading term (u_1, v_1) with characteristic $\lambda_0 = 0$ on time as in the linear theory

$$\begin{pmatrix} u_1 \\ v_1 \end{pmatrix} = A(\tau_1, \tau_2) \begin{pmatrix} A_1 \\ A_2 \end{pmatrix} \cos(q_c x) + B(\tau_1, \tau_2) \begin{pmatrix} A_1 \\ A_2 \end{pmatrix} \cos\left(\frac{q_c x}{2}\right) \cos\left(\frac{\sqrt{3}q_c y}{2}\right), \tag{53}$$

where $A_1/A_2 = [\theta_4 + d_c q_c^2]/\theta_3$, $A(\tau_1, \tau_2)$ and $B(\tau_1, \tau_2)$ are amplitude functions. At $o(\varepsilon^2)$, the equations of (u_2, v_2) are most conveniently written in the vector form

$$\begin{aligned} \tilde{L}_c \begin{pmatrix} u_2 \\ v_2 \end{pmatrix} &= - \begin{pmatrix} \frac{\partial u_1}{\partial \tau_1} \\ \frac{\partial v_1}{\partial \tau_1} \end{pmatrix} - \begin{pmatrix} 0 \\ d_0 \nabla^2 \end{pmatrix} (u_1 \ v_1) + \begin{pmatrix} -\frac{1}{k} \\ 0 \end{pmatrix} u_1^2 \\ &+ \begin{pmatrix} f_1 \\ -f_2 \end{pmatrix} (s_1 u_1^2 - s_3 u_2 v_2 + s_2 v_1^2). \end{aligned}$$

Because the resonant forcing term will appear, this solution is only possible provided a solvability condition, which determines the dependence of A and B on the slow time scale τ_1 . After some algebra, we can obtain the equations of the amplitudes A and B satisfying

$$\begin{cases} E \frac{dA}{d\tau_1} = \gamma_0 A - D_0 B^2, \\ E \frac{dB}{d\tau_1} = \gamma_0 B - 4D_0 AB, \end{cases} \tag{54}$$

where $E > 0$ is constant, $\gamma_0 = A_1 d_0 q_c^2 [\theta_3 + A_2/A_1(\theta_4 - d_c q_c^2)]$, and

$$D_0 = \left[f_1 \theta_3 - f_2 (\theta_4 + d_c q_c^2) \right] p + \frac{\theta_3}{k} A_1^2.$$

The nonresonant forcing solution of $o(\varepsilon^2)$ can be obtained similarly as follows

$$\begin{aligned} \begin{pmatrix} u_2 \\ v_2 \end{pmatrix} &= \begin{pmatrix} p_{11} \\ p_{21} \end{pmatrix} \left(2A^2 \cos(2q_c x) + B^2 \cos(q_c x) \cos(\sqrt{3}q_c y) \right) \\ &+ \begin{pmatrix} p_{12} \\ p_{22} \end{pmatrix} \left(4AB \cos\left(\frac{3q_c x}{2}\right) \cos\left(\frac{\sqrt{3}q_c y}{2}\right) + B^2 \cos(\sqrt{3}q_c y) \right) \\ &+ \begin{pmatrix} p_{13} \\ p_{23} \end{pmatrix} (2A^2 + B^2), \end{aligned}$$

where

$$\begin{aligned} p_{11} &= \frac{Q_1(2q_c)}{4F(0, 2q_c, d_c)}, \quad p_{12} = \frac{Q_1(\sqrt{3}q_c)}{4F(0, \sqrt{3}q_c, d_c)}, \quad p_{13} = \frac{Q_1(0)}{4F(0, 0, d_c)}, \\ p_{21} &= \frac{Q_2(2q_c)}{4F(0, 2q_c, d_c)}, \quad p_{22} = \frac{Q_2(\sqrt{3}q_c)}{4F(0, \sqrt{3}q_c, d_c)}, \quad p_{23} = \frac{Q_2(0)}{4F(0, 0, d_c)} \end{aligned}$$

and the functions F and Q are given in (33) and (36), respectively.

At $o(\varepsilon^3)$, the equations determining (a_3, b_3) become

$$\begin{aligned} \tilde{L}_c \begin{pmatrix} u_3 \\ v_3 \end{pmatrix} = & - \begin{pmatrix} \frac{\partial u_1}{\partial \tau_2} \\ \frac{\partial v_1}{\partial \tau_2} \end{pmatrix} - \begin{pmatrix} \frac{\partial u_2}{\partial \tau_1} \\ \frac{\partial v_2}{\partial \tau_1} \end{pmatrix} - \begin{pmatrix} 0 \\ \bar{d}\nabla^2 v_1 \end{pmatrix} - \begin{pmatrix} 0 \\ d_0\nabla^2 v_2 \end{pmatrix} \\ & + \begin{pmatrix} -\frac{1}{k} \\ 0 \end{pmatrix} u_1 u_2 + \begin{pmatrix} f_1 \\ -f_2 \end{pmatrix} [s_1 u_1 u_2 - s_3 (u_1 v_2 + u_2 v_1) + s_2 v_1 v_2]. \end{aligned}$$

We can determine the equations by the solvability conditions for these amplitude functions of A and B as follows,

$$\begin{cases} E \frac{dA}{d\tau_2} = \gamma_1 A - A (D_1 B^2 + D_2 A^2), \\ E \frac{dB}{d\tau_2} = \gamma_1 B - B [2D_1 A^2 + \frac{1}{4}(D_2 + 2D_1) B^2], \end{cases} \tag{55}$$

where $E > 0$ is a constant, $\gamma_1 = \bar{d}q_c^2[\theta_3 + A_2/A_1(\theta_4 - d_c q_c^2)]$ and

$$D_1 = \zeta [(s_1 - s_3 A_2/A_1)(p_{13} + p_{12}) + (s_2 A_2/A_1 - s_3)(p_{23} + p_{22})] + \frac{\theta_3}{k}(p_{13} + p_{12}), \tag{56}$$

$$D_2 = \zeta [(s_1 - s_3 A_2/A_2)(p_{11} + 2p_{13}) + (s_2 A_2/A_1 - s_3)(p_{21} + 2p_{23})] + \frac{\theta_3}{k}(p_{11} + 2p_{13})$$

with $\zeta = f_2(\theta_4 - d_c q_c^2) - f_1 \theta_3$.

Combining the amplitude equations (54) and (56), we obtain the following general equations

$$\begin{cases} \frac{dA}{d\tau} = \gamma A - D_0 B^2 - A (D_1 B^2 + D_2 A^2) \\ \frac{dB}{d\tau} = \gamma B - 4D_0 AB - B (2D_1 A^2 + \frac{1}{4} (D_2 + 2D_1) B^2), \end{cases}$$

where $\tau = \tau_1 + \tau_2$, $\gamma = (d_0 + \bar{d})q_c^2[\theta_3 + A_2/A_1(\theta_4 - d_c q_c^2)]$, D_0, D_1, D_2 are the Landau constants of the amplitudes A, B . To show that only the terms proportional to $\cos(q_c x)$ and $\cos(q_c x/2) \cos(\sqrt{3}q_c y/2)$ have been retained, which contribute to the hexagonal planform patterns, we catalogue the critical points of these amplitude equations and summarize their orbital stability behavior. Set

$$\gamma_{-1} = \frac{-4D_0^2}{4D_1 + D_2}, \quad \gamma_1 = \frac{16D_0^2 D_2}{(D_2 - 2D_1)^2}, \quad \gamma_2 = \frac{32D_0^2 (D_1 + D_2)}{(D_2 - 2D_1)^2},$$

and obtain the following critical points

- (a) : $A_0 = B_0 = 0$;
- (b) : $A_0^2 = \frac{\gamma}{D_2}, B_0 = 0, (\gamma > 0)$;
- (c $^\pm$) : $2A_0 = B_0 = B_0^\pm = \frac{2[-2D_0 \pm \sqrt{4D_0^2 + \gamma(4D_1 + D_2)}]}{4D_1 + D_2}, (\gamma > \gamma_{-1})$;
- (d) : $A_0 = \frac{4D_0}{D_2 - 2D_1}, B_0^2 = \frac{4(\gamma - \gamma_1)}{D_2 + 2D_1}, (\gamma > \gamma_1)$.

In order to examine the stability of these critical points, we first give the linear matrix $J(A_0, B_0)$ of the critical point (A_0, B_0) ,

$$J(A_0, B_0) = \begin{pmatrix} \gamma - (D_1 B_0^2 + 3D_2 A_0^2) & -2B_0 (D_0 + D_1 A_0) \\ -4B_0 (D_0 + D_1 A_0) & \gamma - 4D_0 A_0 - (2D_1 A_0^2 + \frac{3}{4} (D_2 + 2D_1) B_0^2) \end{pmatrix}.$$

This sort of stability of pattern formation is meant in the sense of a family of solutions in the plane which may interchange with each other but do not grow or decay to a solution type from a different family. Such an interpretation depends upon the translation and rotational symmetries inherent to the amplitude phase equations, the invariance also limits each equivalence class of critical points to a single member that must be considered explicitly. By studying the sign of the eigenvalue σ (where σ is the solution of the equation $|J(A_0, B_0) - \sigma I| = 0$), we obtain that **a** is stable for $\gamma < 0$, while the stability behavior of **b** and \mathbf{c}^\pm which depends upon the signs of D_0 and $2D_1 - D_2$. When **b** is stable, it is again equivalent to our original one-dimensional periodic patterns. The \mathbf{c}^\pm represents two-dimensional periodic patterns exhibiting hexagonal symmetry as in Golubitsky et al. (1984). Finally, the critical point **d**, which reduces to **b** for $\gamma = \gamma_1$ and \mathbf{c}^\pm for $\gamma = \gamma_2$ and hence is called a generalized cell by Wollkind and Stephenson (2000), is not stable for any value of γ .

For the stability of these critical points, we have the following table,

D_0	$2D_1 - D_2$	Stable structures
>0	≤ 0	\mathbf{c}^{-1} for $\gamma > \gamma_{-1}$
>0	<0	\mathbf{c}^{-1} for $\gamma_{-1} < \gamma < \gamma_2$, b for $\gamma > \gamma_1$
$=0$	<0	\mathbf{c}^\pm for $\gamma > 0$
$=0$	>0	b for $\gamma > 0$
<0	>0	\mathbf{c}^+ for $\gamma_{-1} < \gamma < \gamma_2$, b for $\gamma > \gamma_1$
<0	≤ 0	\mathbf{c}^+ for $\gamma > \gamma_{-1}$

Therefore, the stabilities of **b** and \mathbf{c}^\pm are determined by the signs of Landau constants D_0 and $2D_1 - D_2$ and we can simulate the Landau constants for given parameters.

Note that the Turing patterns of **b** represent strip pattern as one-dimensional pattern and the Turing patterns of \mathbf{c}^\pm represent the hexagonal pattern (Wollkind and Stephenson 2000). Consequently, the lowest order solution associated with these critical points of \mathbf{c}^\pm is given by

$$\begin{pmatrix} u - u^* \\ v - v^* \end{pmatrix} \sim A_0^\pm \begin{pmatrix} A_1 \\ A_2 \end{pmatrix} \left[\cos(q_c x) + 2 \cos \frac{q_c x}{2} \cos \frac{\sqrt{3} q_c y}{2} \right], \tag{57}$$

Therefore, we can give the sketch of the Landau constant D_0 and $2D_2 - D_1$ and plot the leading spatial solution as Turing pattern of a hexagonal array of rectangles in (57).

6 Discussion

Since fish provide much of the food base for wading birds, alligators, racoons, and many other animals in the Florida Everglades, it is very important to study the spatiotemporal dynamics of fish in the Everglades and very mathematical models have been proposed for this purpose. For example, [Gaff et al. \(2000, 2004\)](#) used spatially explicit, age-structured models to assess fish density dynamics in the Florida Everglades area based on information concerning fish movement, pond locations, and other field data. [Jopp et al. \(2010\)](#) developed a simple two-patch model to describe the main processes of the spatiotemporal dynamics of a population of small-bodied fish in a seasonal wetland environment, consisting of marsh and permanent waterbodies. To investigate how small fish spread into newly flooded areas and build up substantial biomass in the Florida Everglades, [DeAngelis et al. \(2010\)](#) proposed reaction–diffusion equation models to test two hypotheses: (a) the refuge mechanism which hypothesizes that small remnant populations of small fishes survive the dry season in small permanent bodies of water (refugia), sites where the water level is otherwise below the surface; and (b) the dynamic ideal free distribution mechanism which assumes that consumption by the fish creates a prey density gradient and that fish taxis along this gradient can lead to rapid population expansion in space. By estimating the diffusion rates and numerical simulating, they concluded that the second mechanism, taxis in the direction of the flooding front, seems capable of matching empirical observations. Note that in the model of [DeAngelis et al. \(2010\)](#), the prey (invertebrate) population does not disperse, while the predators (fish) diffuse on an one-dimensional space. To better understand how landscape topography, hydrology, and fish behavior interact to create high densities of stranded fish, [Yurek et al. \(2013\)](#) simulated population dynamics of small fish with different traits for movement strategy and growth rate, across an artificial, spatially explicit, heterogeneous, two-dimensional marsh slough landscape, using hydrologic variability as the driver for movement. Their model output showed that fish with the highest tendency to invade newly flooded marsh areas built up the largest populations over long time periods with stable hydrologic patterns (Figs. 13, 14).

In this paper, we studied a diffusive predator–prey system with Beddington–DeAngelis functional response under homogeneous Neumann boundary conditions which describes the interactions of small fishes and their prey in the Florida Everglades. We considered the local stability of the corresponding ODE system and discussed the uniform bound and global asymptotic stability of the constant steady state of the reaction–diffusion system. Conditions for the local stability and Turing instability of the diffusive model with one-dimensional and two-dimensional domains are given. Finally, we established the amplitude equations of the one-dimensional and two-dimensional patterns and presented the analytical statement of the Landau constants and asymptotic solutions of spatial Turing patterns. Our theoretical results further explain that diffusion of the small fishes and their prey in wetlands ecological systems are an important factor in generating spatial two-dimensional Turing patterns of rhombic and hexagonal planforms. We believe that the existence of two-dimensional rhombic and hexagonal patterns may help us provide additional refugia besides the small ponds and solution holes which maintain tiny populations of small fishes across

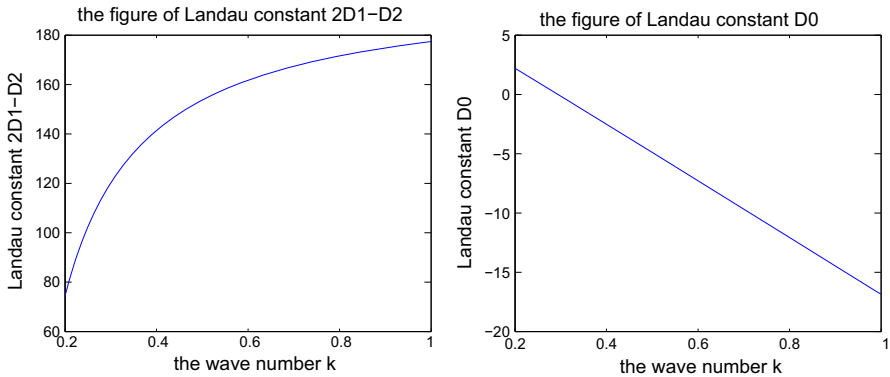


Fig. 13 (Color online) The sketch of Landau constants D_0 and $2D_1 - D_2$

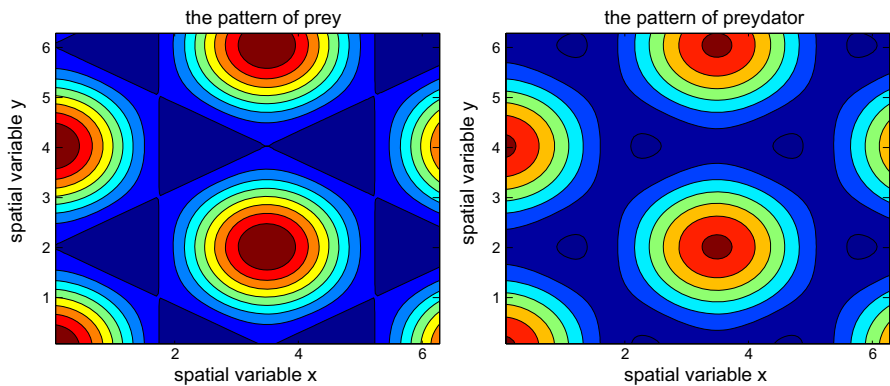


Fig. 14 (Color online) The two-dimensional stable spatial hexagonal patterns

the landscape and thus supports the refuge mechanism. The fact that the interactions between the small fishes and their prey and their dispersal on two-dimensional domains induce two-dimensional rhombic and hexagonal patterns also agree with the modal simulations carried by [Yurek et al. \(2013\)](#).

There has been some work done on patterns of grazers (snails, caddis flies, fish, etc.) and periphyton in streams (see [Blaine and DeAngelis 1997](#); [Kawata et al. 2001](#); [Lamberti and Resh 1983](#); [McIntosh et al. 2004](#)). We think that regular patterns of grazing fish and either invertebrates or periphyton are also possible in the Everglades, which could be done with empirical and numerical studies. We could start with a flat, homogeneous system allow invertebrates to grow and to spread at a slow rate and allow fish to spread more quickly; or else just have the interaction between slowly spreading periphyton and more rapidly moving invertebrate consumers. We will report the empirical and numerical studies somewhere else.

Notice that [Segel and Jackson \(1972\)](#) and [Levin \(1974\)](#) showed that Turing instability may occur in a diffusive predator–prey model if the predators exhibit self-limiting or intraspecific competition. In another words, Turing instability does not occur in

the classical diffusive predator–prey model with Holling type II functional response. However, our result demonstrates that Turing instability could occur in a predator–prey model with Beddington–DeAngelis functional response. On the one hand, this indicates that the self-limiting or intraspecific competition effect of the predators can be relaxed if the predators exhibit mutual interference. On the other hand, this indicates that there are some significant differences between the classical diffusive predator–prey model with Holling type II functional response and the one with Beddington–DeAngelis functional response. As far we know, this difference has not been noticed in any literature.

Ecosystem with regular patterns may be more resilient and resistant to the global environmental change compared to homogeneous ecosystems. This process is key to understanding ecological stability and diversity. We expect further research to better understand the food web and how this affects their response to the Everglades wetland even in a broad spectrum of ecosystems. We also propose to study the spatiotemporal patterns of the predator–prey system with seasonal effect and consider the following model

$$\begin{cases} \frac{\partial I(x,t)}{\partial t} = D_1 \Delta I(x,t) + r \left(1 - \frac{I(x,t)}{K}\right) I(x,t) - \frac{fI(x,t)F(x,t)}{1+hfI(x,t)+wfF(x,t)}, & x \in \Omega, \quad t > 0 \\ \frac{\partial F(x,t)}{\partial t} = D_2(t) \Delta F(x,t) + \frac{\gamma fI(x,t)F(x,t)}{1+hfI(x,t)+wfF(x,t)} - mF(x,t), & x \in \Omega, \quad t > 0, \end{cases} \tag{58}$$

where $D_2(t)$ is periodic with minimum period T . Specifically, we assume that $D_2(t)$ alternates between two constant values; that is,

$$D_v(t) = \begin{cases} D^+ & \text{if } nT < t < (n + \frac{1}{2})T, \\ D^- & \text{if } (n + \frac{1}{2})T < t < (n + 1)T \quad (n \in \mathbb{Z}) \end{cases} \tag{59}$$

where the values of $D_2(nT)$ and $D_2(nT + T/2)$ are irrelevant. The results will help us to understand how small fish invade the wetlands in the Everglades (DeAngelis et al. 2010), the seasonal dynamics of small fish cohorts in the Everglades (Jopp et al. 2010), and how spatiotemporal landscapes are formed in the Everglades as observed in Yurek et al. (2013). We will report the results somewhere else.

Acknowledgements We would like to thank Donald L. DeAngelis for his assistance and input on this project.

References

Alonson D, Bartumeus F, Catalan J (2002) Mutual interference between predators can give rise to Turing spatial patterns. *Ecology* 83:28–34

Andow DA, Kareiva PM, Levin SA, Okubo A (1990) Spread of invading organisms. *Landscape Ecol* 4:177–188

Armstrong PR, Roughgarden JE (2005) The impact of directed versus random movement on population dynamics and biodiversity patterns. *Am Nat* 165:449–465

Aronson DG, Weinberger HF (1975) Nonlinear diffusion in population genetics, combustion, and nerve pulse propagation. In: Goldstein JA (ed) *Partial differential equations and related topics. Lecture notes in mathematics*, vol 446. Springer, Berlin, pp 5–49

- Beddington JR (1975) Mutual interference between parasites or predators and its effect on searching efficiency. *J Anim Ecol* 44:331–340
- Blaine TW, DeAngelis DL (1997) The interaction of spatial scale and predator-prey functional response. *Ecol Model* 95:319–328
- Brown KJ, Dunne PC, Gardner RA (1981) A semilinear parabolic system arising in the theory of superconductivity. *J Differ Equ* 40:232–252
- Cantrell RS, Cosner C (2001) On the dynamics of predator-prey models with the Beddington–DeAngelis functional response. *J Math Anal Appl* 257:206–222
- Cosner C (2005) A dynamic model for the ideal-free distribution as a partial differential equation. *Theor Popul Biol* 67:101–108
- DeAngelis DL, Goldstein RA, O’Neill RV (1975) A model for trophic interaction. *Ecology* 56:881–892
- DeAngelis DL, Trexler JC, Loftus WF (2005) Life history tradeoffs and community dynamics of small fishes in a seasonally pulsed wetland. *Can J Fish Aquat Sci* 62:781–790
- DeAngelis DL, Trexler JC, Cosner C, Obazac A, Jopp F (2010) Fish population dynamics in a seasonally varying wetland. *Ecol Model* 221:1131–1137
- Fisher RA (1937) The wave of advance of advantageous genes. *Ann Eugen* 7:355–369
- Gaff H, DeAngelis DL, Gross LJ, Salinas R, Shorosh M (2000) A dynamic landscape model for fish in the Everglades and its application to restoration. *Ecol Model* 127:33–52
- Gaff H, Chick J, Trexler J, DeAngelis D, Gross L, Salinas R (2004) Evaluation of and insights from ALFISH: a spatially explicit, landscape-level simulation of fish populations in the Everglades. *Hydrobiologia* 520:73–87
- Gawlik DE (2002) The effects of prey availability on the numerical response of wading birds. *Ecol Monogr* 72:329–346
- Golubitsky M, Swift JK, Knoblich Z (1984) Symmetries and pattern selection in Kayleigh–Benard convection. *Phys D* 10:249–276
- Hwang TW (2003) Global analysis of the predator–prey system with Beddington–DeAngelis functional response. *J Math Anal Appl* 281:395–401
- Hwang TW (2004) Uniqueness of limit cycles of the predator–prey system with Beddington–DeAngelis functional response. *J Math Anal Appl* 290:113–122
- Jopp F, DeAngelis DL, Trexler JC (2010) Modeling seasonal dynamics of small fish cohorts in fluctuating freshwater marsh landscapes. *Landsc Ecol* 25:1041–1054
- Kawata M, Hayashi M, Hara T (2001) Interactions between neighboring algae and snail grazing in structuring microdistribution patterns of periphyton. *Oikos* 92:404–416
- Koch AJ, Meinhardt H (1994) Biological pattern formation: from basic mechanisms to complex structures. *Rev Mod Phys* 66:1481–1501
- Lamberti GA, Resh VH (1983) Stream periphyton and insect herbivores: an experimental study of grazing by a caddisfly population. *Ecology* 64:1124–1135
- Levin SA (1974) Dispersion and population interactions. *Am Nat* 108:207–228
- Levin SA, Segel LA (1985) Pattern generation in space and aspect. *SIAM Rev* 27:45–67
- Loftus WF, Kushlan JA (1987) Freshwater fishes of Southern Florida. *Bull Fla State Mus Biol Sci* 31:147–344
- Loftus WF, Johnson RA, Anderson GH (1992) Ecological impacts of the reduction of groundwater levels in short-hydroperiod marshes of the Everglades. In: Stanford JA, Simons JJ (eds) Proceedings of the first international conference on ground water ecology. American Water Resources Association, pp 199–208
- McIntosh AR, Peckarsky BL, Taylor BW (2004) Predator-induced resource heterogeneity in a stream food web. *Ecology* 85:2279–2290
- Murray JD (1993) *Mathematical biology*. Springer, Berlin
- Ni W-M, Tang M (2005) Turing patterns in the Lengyel–Epstein system for the CIMA reaction. *Trans Am Math Soc* 357:3953–3969
- Okubo A, Levin SA (2001) *Diffusion and ecological problems: modern perspectives*. Springer, New York
- Rehage JS, Trexler JC (2006) Assessing the net effect of anthropogenic disturbance on aquatic communities in wetlands: community structure relative to distance from canals. *Hydrobiologia* 569:359–373
- Rietkerk M, van de Koppel J (2008) Regular pattern formation in real ecosystems. *Trends Ecol Evol* 23:169–175
- Segel LA, Jackson JL (1972) Dissipative structure: an explanation and an ecological example. *J Theor Biol* 37:545–549

- Segel LA, Levin SA (1976) Application of nonlinear stability theory to the steady of the effects of diffusion on predator-prey interactions. In: Piccirelli R (ed) Selected topics in statistical mechanics and biophysics. American Institute of Physics Symposium, vol 27, pp 123–152
- Shi HB, Ruan S (2015) Spatial, temporal and spatiotemporal patterns of diffusive predator–prey models with mutual interference. *IMA J Appl Math* 80(5):1534–1568
- Skellam JG (1951) Random dispersal in theoretical populations. *Biometrika* 38:196–218
- Trexler JC, Loftus WF, Jordan CF, Chick J, Kandl KL, McElroy TC, Bass OL (2001) Ecological scale and its implications for freshwater fishes in the Florida Everglades. In: Porter JW, Porter KG (eds) The Everglades, Florida Bay, and Coral reefs of the Florida Keys: an ecosystem sourcebook. CRC, Boca Raton, pp 153–181
- Turing AM (1952) The chemical basis of morphogenesis. *Philos Trans R Soc B* 237:37–72
- Wollkind DJ, Manoranjan VS, Zhang L (1994) Weakly nonlinear stability analyses of prototype reaction-diffusion model equations. *SIAM Rev* 36:176–214
- Wollkind DJ, Stephenson LE (2000) Chemical Turing pattern formation analysis: comparison of theory with experiment. *SIAM J Appl Math* 61:384–431
- Yan X-P, Zhang C-H (2014) Stability and Turing instability in a diffusive predator–prey system with Beddington–DeAngelis functional response. *Nonlinear Anal Real World Appl* 20:1–13
- Yurek S, DeAngelis DL, Trexler JC, Jopp F, Donalson DD (2013) Simulating mechanisms for dispersal, production and stranding of small forage fish in temporary wetland habitats. *Ecol Model* 250(2013):391–401
- Zhang X-C, Sun G-Q, Jin Z (2012) Spatial dynamics in a predator–prey model with Beddington–DeAngelis functional response. *Phys Rev E* 85:021924